

Changing dynamics of urban biophysical composition and its impact on urban heat island intensity and thermal characteristics: the case of Hyderabad City, India

Srikanta Sannigrahi¹ · Shahid Rahmat¹ · Suman Chakraborti² · Sandeep Bhatt³ · Shouvik Jha⁴

Received: 31 January 2017 / Accepted: 5 May 2017 / Published online: 22 May 2017
© Springer International Publishing Switzerland 2017

Abstract The biophysical composition; including the green surface cover and moisture dynamics substantially affects the thermal character and Surface Urban Heat Island intensity (SUHI) of an urban area. Therefore, biophysical indices are highly sensitive to the changing process in land use and land cover. Remote sensing based land surface temperature (LST) plays a significant role in analyzing the thermal behavior of urban areas at multiple scales to moderate the urban heat island. In the present study, Greater Hyderabad Municipal Corporation, is taken as a case study to assess biophysical controls on LST and UHI in an urban ecosystem by implementing biophysical indices. Therefore, the cluster of UHI and the proximity to the hotspots were created from spatial statistics. The areal coverage of urban land was increased from 31.2% in 1973 to

62.87% in 2015 with 5.03 sq km year⁻¹ expansion rate. The LST hotspot (H–H) in 2002 observed in the central and the southeast portion of the region, ascribe to the presence of higher thermal anomalies, whereas, the mean LST (°C) of the neighboring region is below than the average. The highest negative correlation between the estimated LST (°C) and the biophysical indices was accounted over aquatic vegetation cover, followed by urban green spaces and built-up urban area, respectively. The simple linear and multiple regression models demonstrated the complex and nonlinear behavior of the UHI and LST with the biophysical components. Therefore, the spatial coherence among the biophysical indices with LST ensembles the necessity of urban greenery and parks within the urban counterpart to mitigate the outdoor thermal discomfort to a reasonable extent.

✉ Srikanta Sannigrahi
srikanta.arp@iitkgp.ac.in

Shahid Rahmat
shahidrahmat82@arp.iitkgp.ernet.in

Suman Chakraborti
suman87_ssf@jnu.ac.in

Sandeep Bhatt
sandeep@gg.iitkgp.ernet.in

Shouvik Jha
shouvik.jha@iccsir.org

¹ Department of Architecture and Regional Planning, Indian Institute of Technology, Kharagpur, West Bengal, India

² Center for the Study of Regional Development (CSRD), Jawaharlal Nehru University, New Delhi, India

³ Department of Geology and Geophysics, Indian Institute of Technology, Kharagpur, West Bengal, India

⁴ Indian Centre for Climate and Societal Impacts Research (ICCSIR), Mandvi, Kachchh, Gujarat, India

Keywords LST · SUHI · Biophysical indices · Thermal comfort · Spatial statistics · Urban ecosystem

Introduction

Urban Heat Island (UHI) problem now becomes a global phenomenon affecting the city's climate and its environmental quality to a larger extent (Voogt and Oke 2003; Chudnovsky et al. 2004). The magnitude of air and earth surface temperature difference between cities and its suburban is collectively defined as UHI (Landsberg 1981; Weng et al. 2004) or urban heat archipelago if the structure is multicellular in nature which could probably occur at the first part of the night (Bottyan and Unger 2003). Oke (1987) classified the UHI by two types: canopy layer UHI (consist with the rough air temperature of tree canopy and building with an upper boundary situated just below the roof level) and boundary layer UHI (it is located above the

canopy layer, where the lower boundary influencing urban surface temperature) (Weng et al. 2004). Highly urbanized impervious surface could alter the biophysical compositions which could modify the physical process of earth-atmosphere energy exchange (Oke 1987). UHI studies have directed into two distinct way since the beginning of its application on urban climatic studies: (1) quantifying UHI phenomenon of a particular air parcel based on automobile transect and in situ weather network measurement, and (2) measuring earth surface temperature through the use of satellite remote sensing observation (Streutker 2003).

The changing dynamics of land use and land cover brought by human activity at any ecosystem scale seems to have incremental and unconscious, could lead to an undesirable modification of the native environment (Carlson and Arthur 2000). The unusual changes in land use and expansion of urbanized surface could substantially decrease half of the diurnal temperature range and could warm the mean earth surface temperature by 0.27 °C per century (Kalnay and Cai 2003). In addition, the sensitivity of land use and land cover changes and earth surface temperature found to be zero or close to zero in globally, however, the dynamics of land surface temperature, precipitation, and other climate components can be as large as or greater than those that result from the anthropogenic increase of well-mixed greenhouse gases (Pielke 2005). Moreover, the immediate effects of environmental changes are more prominent at regional and local scale than that of globally averaged values (Pielke 2005). It is also evident that long run land use changes by the human may have decreased the air temperature by 1–2 °C at mid-latitude agricultural region and could be warming by 1–2 °C in the deforested tropical region and extratropical region due to teleconnection process (Fedema et al. 2005). UHI phenomenon could be the extreme case of land use alteration at regional and local scale, where the unprecedented changes of vegetation cover, impervious surface area, and complex geometry of building in an urban landscape lowering the evaporative cooling, store the excess heat and hence, warm the earth surface (Foley et al. 2005). Likewise, Yue et al. (2007), Chen et al. (2006) reported that UHI intensity level is closely associated with the landscape pattern, i.e. composition and configuration of land use and land cover (LULC), the abundance of green cover, extent of impervious (Deng and Wu 2013b) surface and their changes and correlation of spatial metrics with urban heat island is helpful to determine the spatial change of land use classes and associated changes in surface temperature. Therefore, the detail investigation of long run LULC changes at any ecosystem scale could help us to explain the discrepant and unprecedented modification of earth surfaces, and also contribute to describing the directions and degree of other human-related environmental changes (Xiao and Weng 2007; Zeng et al. 2015a, b).

There is a substantial evidence of using remote sensing based biophysical indices to examine the thermal heat island phenomenon (Streutker 2003; Weng et al. 2004, 2007; Chen et al. 2006; Zhang et al. 2009; Amiri et al. 2009). NDVI was used in conjunction with soil-vegetation-atmospheric-transfer (SVAT) model to ascertain the surface soil moisture variability and fraction of vegetation cover (FVC) (Carlson et al. 1994), which can used for estimating leaf area index (LAI), surface impervious fraction, biomass and crop yield (Carlson and Ripley 1997). Weng et al. (2004) studied UHI intensity by investigating the applicability of vegetation fraction estimated from the linear spectral unmixing model as potential indicators of vegetation abundance. Recent studies have been giving thrust on dynamics of the biophysical indicator in response to changing urban heat island to measure the sustainability of an urban area and living conditions within the city. Besides, the selected biophysical descriptors are found highly correlated with land surface temperature (LST) in pearl river delta (PRD) in Guangdong Province, southern China, where NDVI, LSWI, and NDBaI were negatively associated with LST, NDBI was positively correlated with temperature (Chen et al. 2006). However, the correlation between LST and NDVI values related to different land-use types are significantly different (Yue et al. 2007). Yuan and Bauer (2007) analyzed the usability of NDVI and the impervious surface fraction as indicators of SUHI effects by examining the correlation between the LST, impervious surface fraction, and the NDVI. The similar observation has been made by Zhang et al. (2009), where the correlations between NDVI and LST are rather weak than that of the relationship between percent ISA, NDBI, and LST. This suggests that percent ISA, combined with LST, and NDBI, can quantitatively describe the spatial distribution and temporal variation of urban thermal patterns and associated LULC conditions.

The application of thermal remote sensing is considered the most feasible way to examine and characterizing the urban ecosystem at any ecosystem scale. Amiri et al. (2009), Chun and Guldmann (2014), Deng and Wu (2013a, b, c), Ishola et al. (2016), Ayanlade, (2016), Kayet et al. (2016), Sahana et al. (2016) have been used the multi-temporal Landsat 4 multi-spectral scanner (MSS), 5 thematic mapper (TM) and Landsat 7 enhanced thematic mapper (ETM+) sensors for estimating spatiotemporal LST and UHI. Buyantuyev and Wu (2010) was used the spectral and thermal data of advanced spaceborne thermal emission and reflection radiometer (ASTER) to examine the spatially explicit patterns of Phoenix's SUHI. Cao et al. (2010) have also been used moderate resolution ASTER and fine resolution IKONOS data to quantify park cool island intensity (PCI). Therefore, the best advantage of incorporating the

geospatial information to evaluate the status of an urban climatic phenomenon is its easy availability and economic viability.

In the present study, Greater Hyderabad Municipal Corporation (GHMC) is our study boundary, despite the uses of surroundings area. The planning for future sustainable area come under the administrative boundary and moreover, Hyderabad is the capital city of Andhra Pradesh, and the population growth is continuously increasing. Therefore, the study insists on assessing biophysical controls on LST and UHI in an urban ecosystem by implementing biophysical indices (Fig. 1). The discrepant impact of LULC changes and biophysical descriptors on UHI intensity of an urban ecosystem has been evaluated using thermal remote sensing data. Five distinct UHI intensity classes were generated using the relative brightness temperature approach and were deployed to assess the spatial cluster of UHI hot spot and cold spot. The simple linear and multiple regression models were demonstrated the complex and nonlinear behavior of the UHI and LST with the biophysical components. Therefore, the spatial coherence among the biophysical

indices with LST ensembles the necessity of urban greenery and parks within the urban counterpart to mitigate the outdoor thermal discomfort to a reasonable extent.

Methods and data

Land surface temperature (LST) is the radiative temperature of the earth surface which plays a significant role in the physics of earth surface processes through the exchanges of water and energy with the atmosphere (Zhang et al. 2009). The thermal infrared spectrum (10.44–12.42 μm) of 16 days Landsat and 8 days composite of MODerate Resolution Imaging Spectroradiometer (MODIS) satellite data were used for the retrieval of land surface temperature in 2002, 2008, 2011 and 2015, respectively (Weng et al. 2004). The thermal band of Thematic Mapper (TM) having the spatial resolution of 120 m was further resampled onto 60 m for spatial adjustment with the enhanced thematic mapper (ETM+) data. The ETM+ data has been well calibrated in different training locations across the world with a negligible bias (Arvidson 2002). Landsat-based

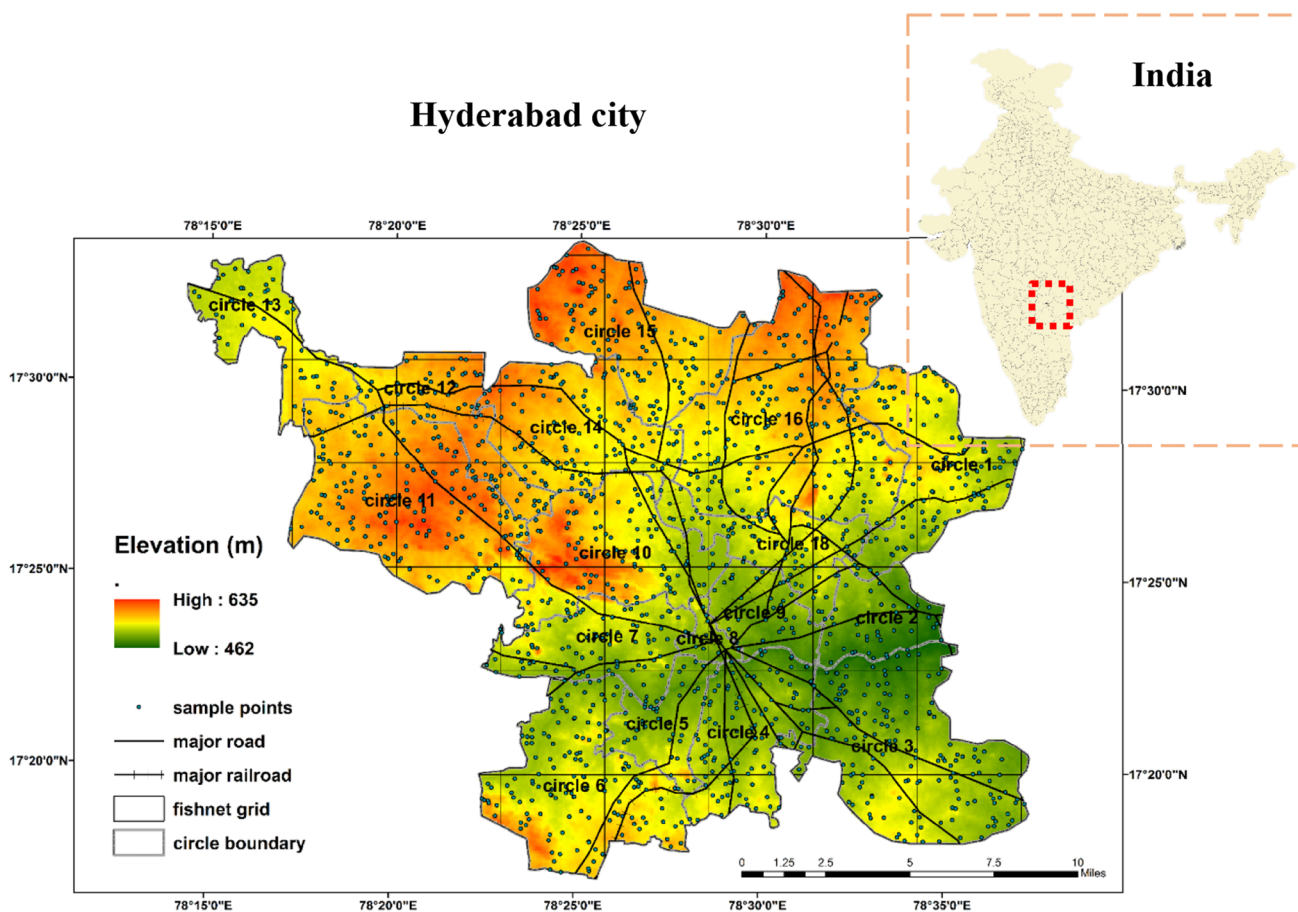


Fig. 1 Location of Greater Hyderabad Municipal Corporation (GHMC), with elevation and major transportation of the city

LST was estimated as follows: (1) converted the digital number (DN) of thermal bands into absolute units of top-of-atmospheric (TOA) radiance; (2) converted the top-of-atmospheric radiance to at-satellite brightness temperature; and (3) converted the at-satellite brightness temperature to earth surface temperature (Barsi et al. 2003; Li et al. 2011). Firstly, the actual DN's of each thermal band was converted to spectral radiance as follows:

$$L_y = \left(\frac{L_{\max} - L_{\min}}{Qcal_{\max} - Qcal_{\min}} \right) \times Qcal - Qcal_{\min} + L_{\min} \quad (1)$$

where L_y is the at satellite spectral radiance, L_{\max} and L_{\min} are the spectral radiance of band 6 at maximum, $Qcal_{\max}$ and $Qcal_{\min}$ are 255 and 1 respectively and $Qcal$ is the DN value of thermal band. For TM, L_{\max} and L_{\min} are 15.303 [Watts/(m² sr μm)] and 1.238 [Watts/(m² sr μm)], and for ETM+, the values are b_{61} : 17.040 [Watts/(m² sr μm)] and 0 [Watts/(m² sr μm)]; b_{62} : 12.650 [Watts/(m² sr μm)] and 3.2 [Watts/(m² sr μm)]. For Landsat 8, the equation can be followed:

$$L_y = ML \times Qcal + AL \quad (2)$$

where ML : (3.3×10^{-04}) and AL : (0.1) are the band-specific multiplicative rescaling factor and band-specific additive rescaling factor of b_{10} and b_{11} , $Qcal$ is the calibrated pixel values (DN). Afterward, at-satellite spectral radiance was converted into at-satellite brightness temperature as follows:

$$T_b = \frac{K_2}{\ln[(K_1/L_y) + 1]} \quad (3)$$

where T_b is the at-satellite brightness temperature (K), K_1 and K_2 are the prelaunch calibrations constant in [Watts/(m² sr μm)] and Kelvin, respectively. For Landsat TM, K_1 and K_2 are: 607.76 [Watts/(m² sr μm)] and 1260.56 K. For Landsat ETM+, K_1 and K_2 are 666.09 [Watts/(m² sr μm)] and 1282.71 K. For Landsat 8, K_1 and K_2 are 774.89 [Watts/(m² sr μm)] and 1321.08 K for band 10 and 480.89 [Watts/(m² sr μm)] and 1201.14 K for band 11 respectively. (Chander et al. 2009; Zhang et al. 2009; Chander and Markham 2003).

Finally, LST was retrieved after converting the at-satellite brightness temperature (K) to land surface temperature (LST) as follows:

$$T_s = \frac{T_b}{[1 + (\lambda T_b / \rho) \ln \varepsilon]} - 273.15 \quad (4)$$

where T_s is at surface temperature (°C), λ is the wavelength of radiance (for which the peak response attain) (11.5 μm was used here), ε is the surface emissivity.

$$\rho = h \times (c / \sigma)$$

where h = Planck's constant (6.626×10^{-34} Js), c = velocity of light (2.998×10^8 m/s⁻¹), σ = Boltzmann constant (1.38×10^{-23} J/K). $\rho = 14,380$ used in this study (Weng et al. 2004; Markham and Baker 1985; Snyder et al. 1998).

$$\begin{aligned} \varepsilon_{TM} &= 0.004P_v + 0.986 \\ \varepsilon_{ETM+L8} &= 0.02644P_v + 0.96356, \end{aligned} \quad (5)$$

where P_v = fractional vegetation cover can be extracted as follows:

$$P_v = \left[\frac{NDVI - NDVI_{\min}}{NDVI_{\max} - NDVI_{\min}} \right]^2 \quad (6)$$

$$NDVI_{TM,ETM+} = \frac{\rho_4 - \rho_3}{\rho_4 + \rho_3} \quad (7)$$

$$NDVI_{L8} = \frac{\rho_5 - \rho_4}{\rho_5 + \rho_4} \quad (8)$$

where $NDVI$ = normalized difference vegetation index, ρ_3 , ρ_4 and ρ_5 are the spectral bands of Landsat TM, ETM+ and Landsat 8, respectively. $NDVI_{\max} = 0.5$ and $NDVI_{\min} = 0.2$. (Sobrino et al. 2004).

Four major biophysical indices, i.e. NDVI, LSWI, NDBI, and NDBaI were considered to examine the impact of urban landscape composition on surface heat island intensity and thermal changes. As the built-up and green surface have very high reflectance within the near infrared spectrum and very low reflectance in visible spectrum, the extent of built-up and green surface coverage have been measured using the reflectance values of three infrared bands (b_4 , b_5 , and b_6) and one visible band (b_3) (Xiao et al. 2001) as follows:

$$LSWI = \frac{\rho_4 - \rho_5}{\rho_4 + \rho_5} \quad (9)$$

$$NDBI = \frac{\rho_5 - \rho_4}{\rho_5 + \rho_4} \quad (10)$$

$$NDBaI = \frac{\rho_5 - \rho_6}{\rho_5 + \rho_6}, \quad (11)$$

where $LSWI$ land surface water index, $NDBI$ normalized difference built-up index, and $NDBaI$ normalized difference bareness index (Zha et al. 2003; Jackson et al. 2004; Maki et al. 2004; Zhao et al. 2005; Xu 2006; He et al. 2010).

Urban heat island effects considered as a relative phenomenon of thermal discrepancies between the urban and its suburban counterpart. The earlier study established a good correlation between the infrared and surface temperature over urban areas could be attributed reliable predictors

of SUHI. The relative brightness temperature approach proposed by Xu et al. 2013 was used in this study to quantify the UHI in GHMC region as follows:

$$T_R = \frac{T_i - T_a}{T_a}, \tag{12}$$

where the relative brightness temperature (K) is T_R , T_i is the brightness temperature at one place, and T_a is the average brightness temperature of the region.

The spatial coherence between the estimated biophysical indices and LST has been assessed through standard model validation statistics: coefficient of determination (R^2), correlation coefficient (r), root mean square error (RMSE) and bias.

$$R^2 = 1 - \frac{\sum (X_i - Y_i)^2}{\sum Y^2 - \frac{\sum Y^2}{N}} \tag{13}$$

$$r = \frac{\sum xy}{\sqrt{\sum x^2 \sum y^2}} \tag{14}$$

$$RMSE = \sqrt{\sum_{i=1}^n (y_i - \hat{y}_i)^2} \tag{15}$$

$$Bias = \frac{\sum_{i=1}^n (y_i - \hat{y}_i)}{n}, \tag{16}$$

where x and y is the explanatory and response variables, \hat{y} is the y predicted, n is the total no. of observation.

Results

LULC dynamics from 1973 to 2015

LULC of the study area were analyzed for the year 1973, 2002, 2011 and 2015 are presented in Fig. 2. For the period of 1973 to 1991, maximum changes (37.38–11.45%) has been observed in the urban green space class. This category of LULC has a large negative change (–25.93% percentage point/pp), followed by farmland (17.12–37.38%) urban built-up (31.2–33.92%), aquatic vegetation, (7.65–9.73%), fallow land (4.12–5.66%) and water body (2.53–1.86%), respectively. Second largest change in this period is in farmland. This category of LULC has a large positive change (+20.26% pp) (Fig. 2; Table 1). Looking at the period of 1973 to 2015 together, aquatic vegetation cover changed from 7.65 to 10.18% (+2.53 pp), followed by water body [2.53–1.33% (–1.2 pp)], urban built-up [31.2–62.87% (31.67 pp)], farmland [17.12–5.17% (–11.95

pp)], fallow land [4.12–14.3% (10.18 pp)] and urban green space [37.38–6.15% (–31.23 pp)], respectively. The largest change in this period is in urban built-up. This category of LULC has a large positive change (–31.67 pp) in the period of 1973 to 2015. Second most significant change in this period is in urban green space. This category of LULC has a large negative change (–31.23 pp) (Fig. 2; Table 1). The multidirectional expansion of built-up urban surface from 1973 to 2015 derived from Landsat images are shown in Fig. 3. The maximum expansion is accounted towards the south-east and northwest direction of the study area. After that, the three major socioeconomic variables, i.e. population distribution, population density and settlement density have been evaluated and tried to correlate with UHI intensity. The highest population density was observed in 4, 5, 8, 9 circles, while settlement density is highest in 7 and 8th circles of the city (Fig. 4). LULC transformation between different classes has been assessed for two different periods, 1991 to 2015 and 2002 to 2015, respectively (Fig. 5).

LST and UHI dynamics across the study region

Spatio-temporal variation of mean air temperature was analyzed for the month of January in the years 1991, 2002 and 2015. There is a very clear pattern of higher mean air temperature in the southeasterly direction to lower mean air temperature in the NW direction in the study area. In the study period (1991–2015), there is a gradual increase in the coverage of higher mean air temperature from southeast direction to the central part and towards northwest direction. Looking at the LULC map, urban built up class reveals the similar pattern of increase in coverage over time (Fig. 6). The estimated land surface temperature was measured for the year 2002, 2011 and 2015 in the month of October are shown in Fig. 7. For the year 2002, the observed minimum temperature for different LULC class varies between 16.1 °C (built-up land) to 18.9 °C (water body). In the same year, for various LULC classes, maximum temperature varies between 28.3 °C (water body) to 34.8 (built-up land). Furthermore, in the year of 2011, considering different LULC classes, the minimum temperature varies between 12.8 °C (built-up area) to 21.9 °C (water body) while, the maximum temperature ranges from 29.1 °C (water body) to 34.1 (farmland). Besides, in 2015, for different LULC class minimum temperature varies between 18.7 °C (built-up land) to 19.7 °C (farmland), while concerning different LULC classes, maximum temperature ranges from 26.8 °C (water body) to 33.6 (built-up land) across the study region. There is a trend of increase in minimum temperature in the period of 2002 to 2015. The result showed that the estimated minimum temperature of different LULC (aquatic vegetation (16.3–19.1 °C), built-up

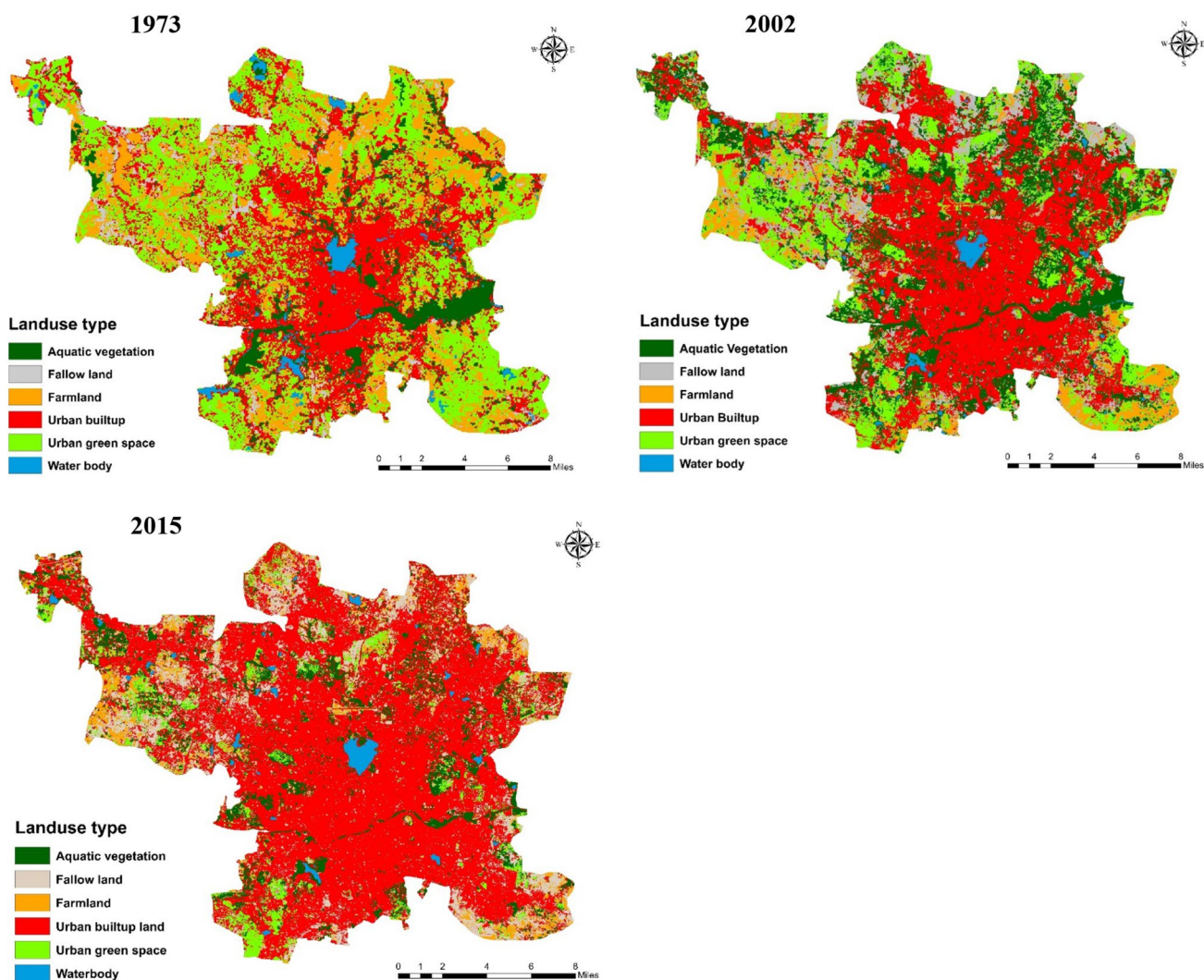


Fig. 2 Land use land cover change dynamics in Hyderabad city during 1973–2015

land (16.1–18.7 °C), farmland (17.1–19.7 °C), fallow land (16.5–19.4 °C) and green space (16.6–19.0 °C)] changes sharply. An exception to this trend is water body, which remained at 18.9 °C in this period but with very high fluctuation in temperature (21.9 °C) in the year 2002 (Fig. 7; Table 2). However, results showed that there is a general trend of decrease in maximum temperature in the period of 2002 to 2015, found maximum over the areas occupied by aquatic vegetation cover, (34.3–31.2 °C), followed by water body (28.3–26.8 °C), built-up land (34.8–33.6 °C), farm land (33.1–30.9 °C) and fallow land (33.5–31.8 °C) (Fig. 7; Table 2). The exception to this trend is urban green space, which increased from 32.9–33.4 °C in this period but with a peak temperature of (34.0 °C) in the year 2002. The UHI Intensity for the year of 2002 (–0.61 to 0.37), 2011 (–0.51 to 0.45) and 2015 (–0.28 to 0.28)

have been calculated and are shown in Fig. 8. The resulting five distinct UHI intensity classes, i.e. green island, weak heat island, medium heat island, strong heat island, and very strong heat island are being discussed in Fig. 9 and Table 3 with addressing the spatial heterogeneity and temporal discrepancies of transforming the thermal cluster of the region from cool spot or atoll to hot spot or island. Only southeastern and eastern part of the area converted to the cool island with time, while, the most of the region are being transformed into strong and extremely heat island during 2002–2015. Four different transects (North, South, East and West), are drawn from the center up to 10 km to examine the UHI sensitivity and thermal differences between the urban CBD and its rural counterpart for the year 1991, 2002, 2011 and 2015, respectively (Fig. 10).

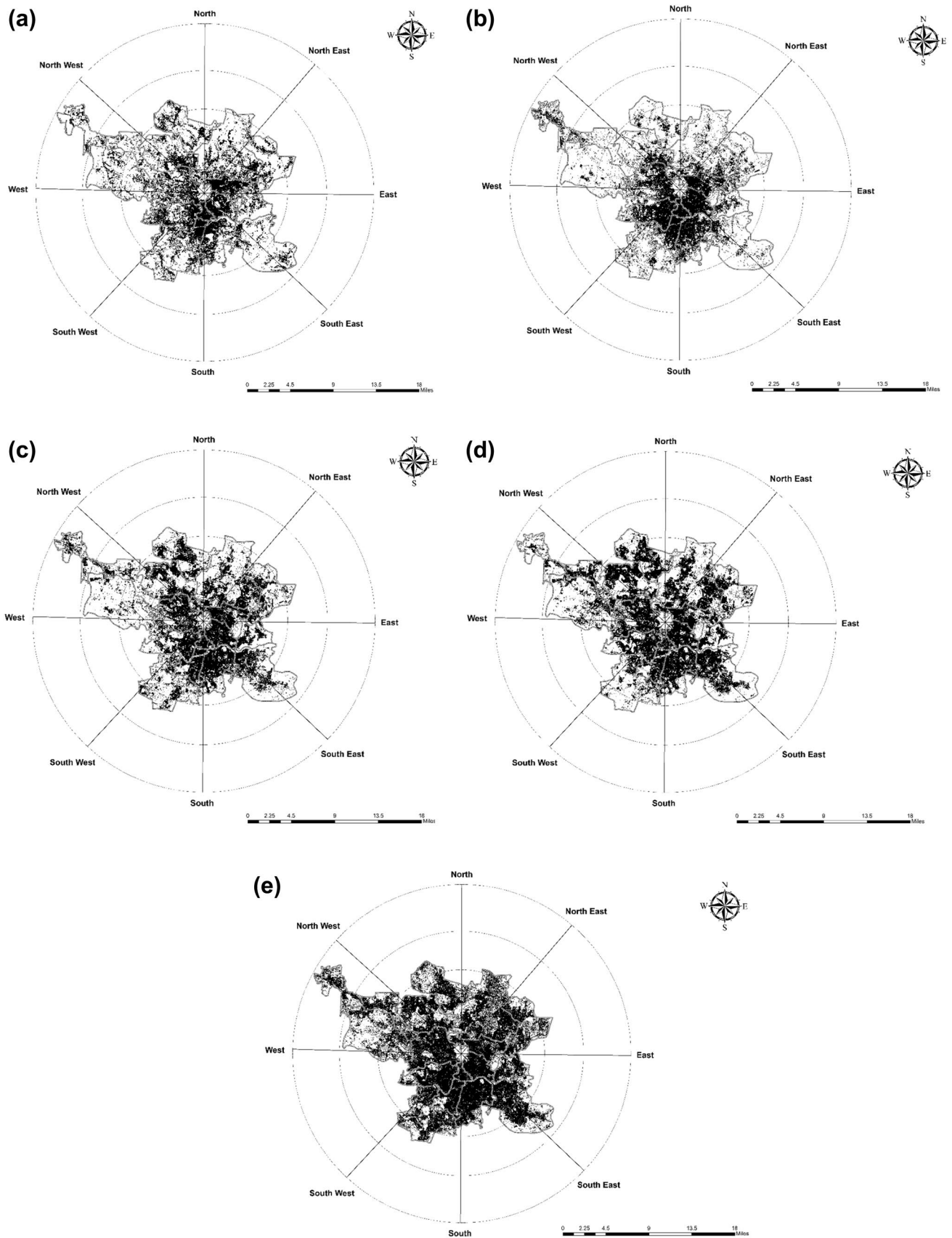


Fig. 3 Spatiotemporal dynamics of impervious surface in **a** 1973, **b** 1991, **c** 2002, **d** 2011 and **e** 2015 extracted from Landsat Satellite imagery

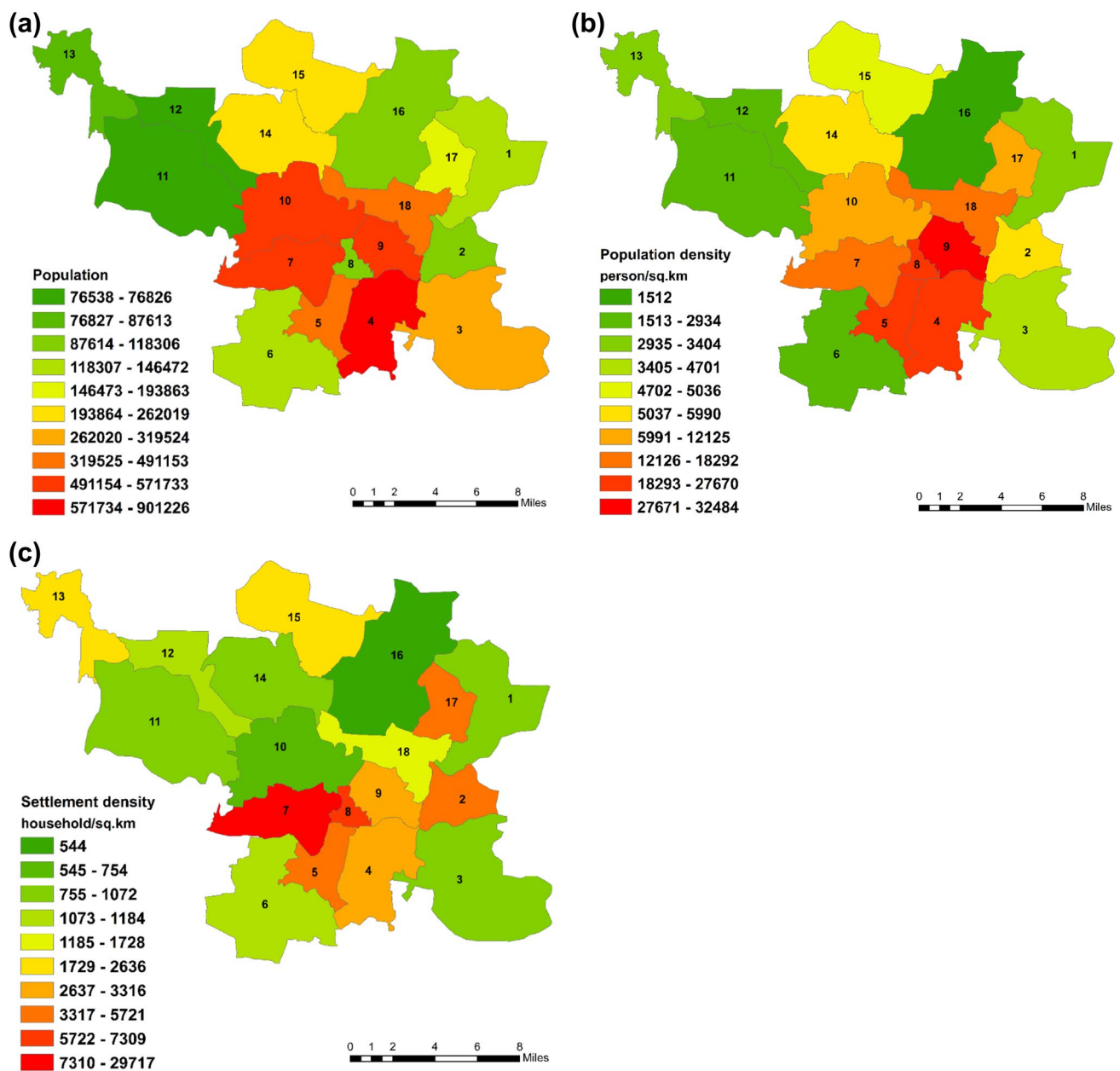


Fig. 4 Spatial variation of the socioeconomic variables; i.e. **a** distribution of population, **b** population density and **c** settlement density in Hyderabad city

Dynamics of biophysical indices across the study region

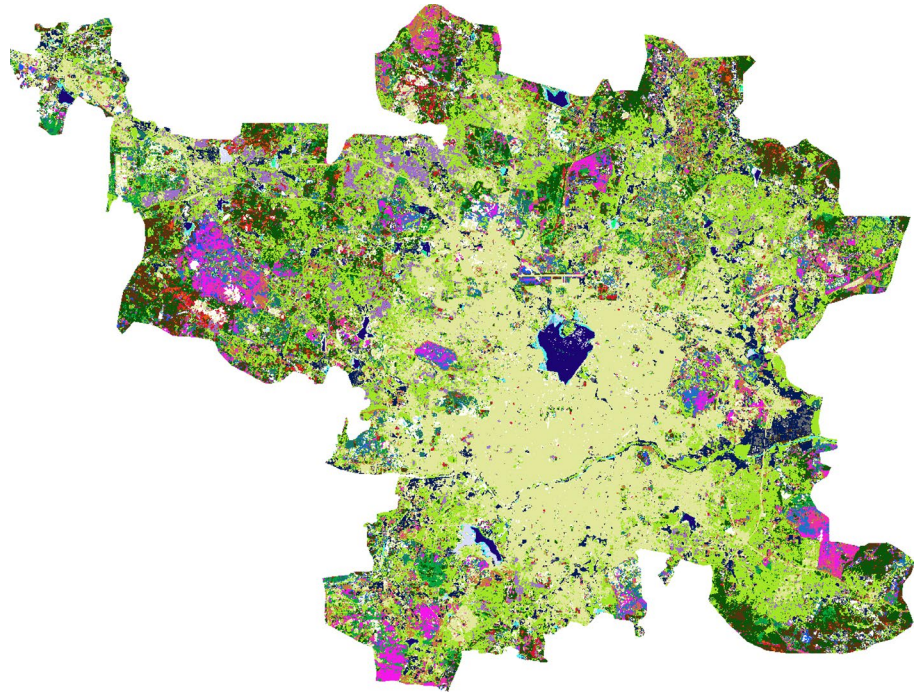
Spatio-temporal variation of LSWI was analyzed for the month of September. There is a gradual change in the coverage of medium-higher values of LSWI to lower values of LSWI. This shift is prominent in the central to south-central part of the study area. This change is also evident in central to northern part of the study area, but in a scattered manner (Fig. 11). NDVI and NDBI have followed the similar tendencies as the minimum values are highly concentrated over built-up areas.

The coefficient of determination and person correlation coefficient test was done between the explanatory (biophysical variables) and response (LST). The coefficient of regression between NDVI for farmland (−152.23, 76.32), A. vegetation (12.24), urban built up (−8.01), fallow land (−7.74, 3.7) and urban green space (−4.72) and LST are in decreasing order (absolute value) and was found to be negative considering all LULC classes. The similar tendencies were observed while testing the spatial and temporal coherence between LSWI for farmland (−26.01), urban built up (−17.66), A. vegetation (−11.11), urban green space

LULC conversion during 1991 - 2015

- Aqua veg to Fallow
- Water to Fallow
- Fallow to Fallow
- U green to Fallow
- Farm to Fallow
- Aqua veg to Built-up
- Water to Built-up
- Builtup to Built-up
- Fallow to Built-up
- U green to Built-up
- Farm to Built-up
- Water to Aqua veg
- Fallow to Aqua veg
- U green to Aqua veg
- Farm to Aqua veg
- Water to Water
- Water to Farm
- Fallow to Farm
- U green to Farm
- Farm to Farm
- Water to U green
- Fallow to U green
- U green to U green
- Farm to U green

1991 - 2015



LULC conversion during 2002 - 2015

- Aqua veg to Fallow
- Water to Fallow
- Fallow to Fallow
- Farm to Fallow
- U Green to Fallow
- Aqua veg to Built-up
- Water to Built-up
- Built-up to Built-up
- Fallow to Built-up
- Farm to Built-up
- Aqua veg to Aqua veg
- Water to Aqua veg
- Fallow to Aqua veg
- Farm to Aqua veg
- Water to Water
- Farm to Water
- Aqua veg to Farm
- Water to Farm
- Fallow to Farm
- Farm to Farm
- Aqua veg to U green
- Water to U green
- Fallow to U green
- Farm to U green
- U green to U green

2002 - 2015

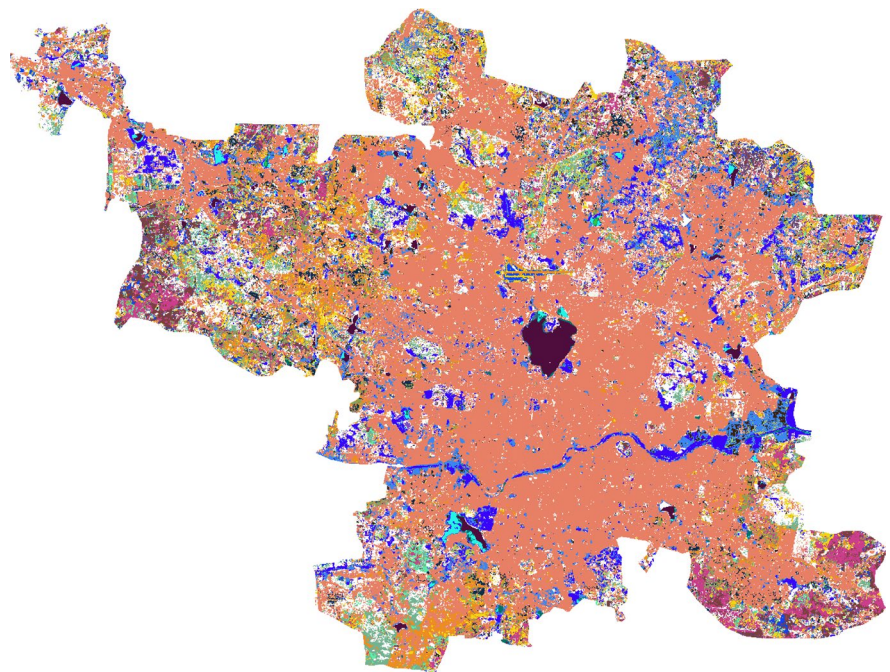
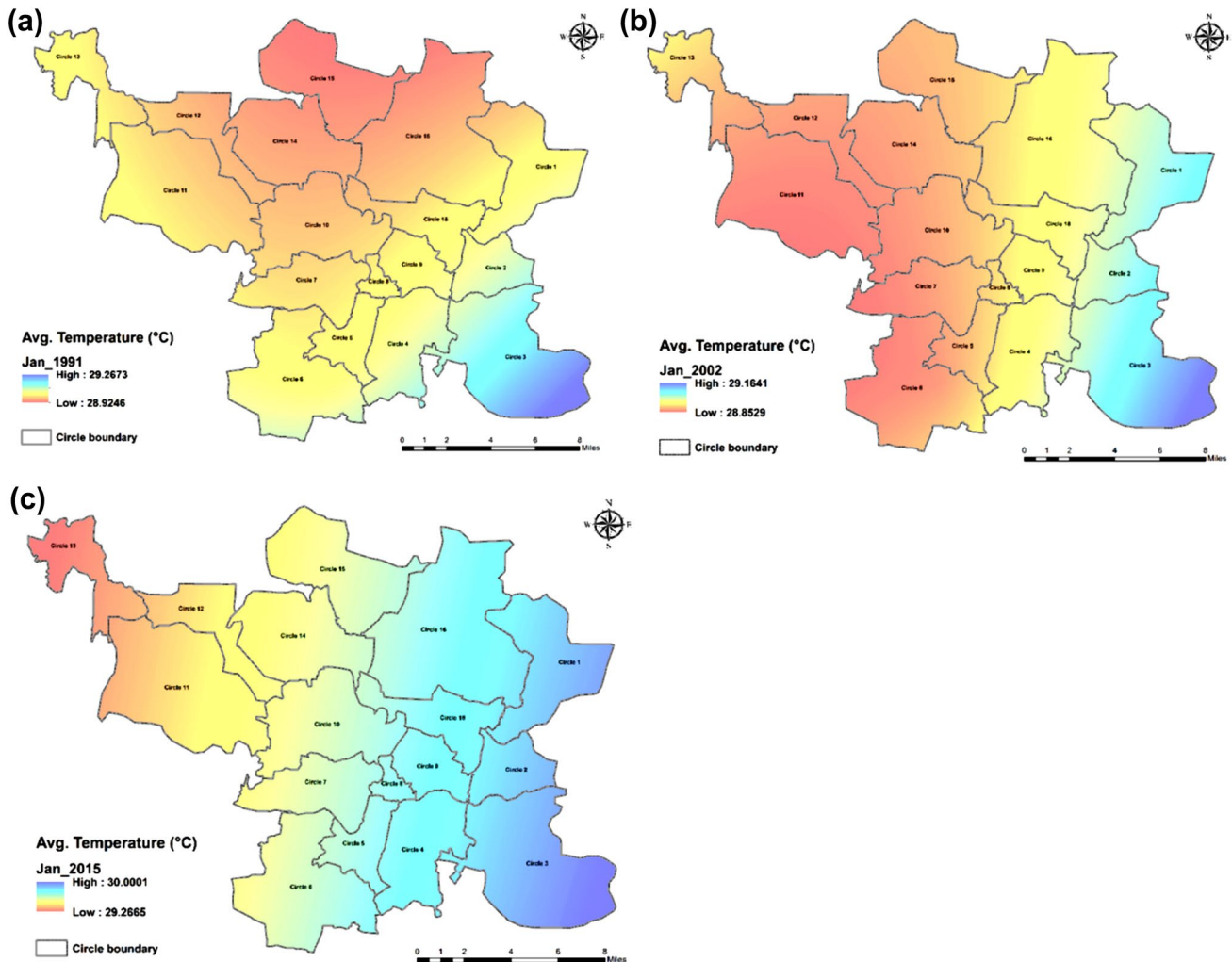


Fig. 5 LULC conversion during 1991–2015 and 2002–2015 in GHMC

Table 1 LULC dynamics in the GHMC during 1973–2015 (unit = %)

LULC	1973	1991	Change	2002	Change	2011	Change	2015	Change	Final change
A. vegetation	7.65	9.73	2.08	21.3	11.57	27.89	6.59	10.18	-17.71	2.53
Water body	2.53	1.86	-0.67	1.18	-0.68	1.36	0.18	1.33	-0.03	-1.2
Urban built-up	31.2	33.92	2.72	41.35	7.43	45.99	4.64	62.87	16.88	31.67
Farmland	17.12	37.38	20.26	6.2	-31.18	3.78	-2.42	5.17	1.39	-11.95
Fallow land	4.12	5.66	1.54	11.71	6.05	3.65	-8.06	14.3	10.65	10.18
U green space	37.38	11.45	-25.93	18.27	6.82	17.33	-0.94	6.15	-11.18	-31.23
Total	100	100		100		100	0	100		

**Fig. 6** Spatio-temporal variation of mean air temperature (°C) in **a** 1991, **b** 2002, and **c** 2015

(-10.10) and fallow land (-9.42) with LST. The absolute value found to be decreased with time. The correlation was done between LST and NDBaI for farmland (30.00), A. vegetation (-27.78), urban green space (-25.98), urban built up (-25.62) and fallow land (9.12) are also found in decreasing order (absolute value) (Table 4). However, the coefficient of regression was found to be positive between

LST and NDBI for all the LULC classes, while the absolute value follows the declining trend [farmland (24.89), urban built up (17.45), A. vegetation (10.94), fallow land (10.75) and urban green space (4.81)] (Figs. 12, 13). The sensitivity between the LST and the biophysical indices (NDVI, LSWI, NDBI, and NDBaI) are shown in Fig. 14. Fallow land is found to be most sensitive in the response of

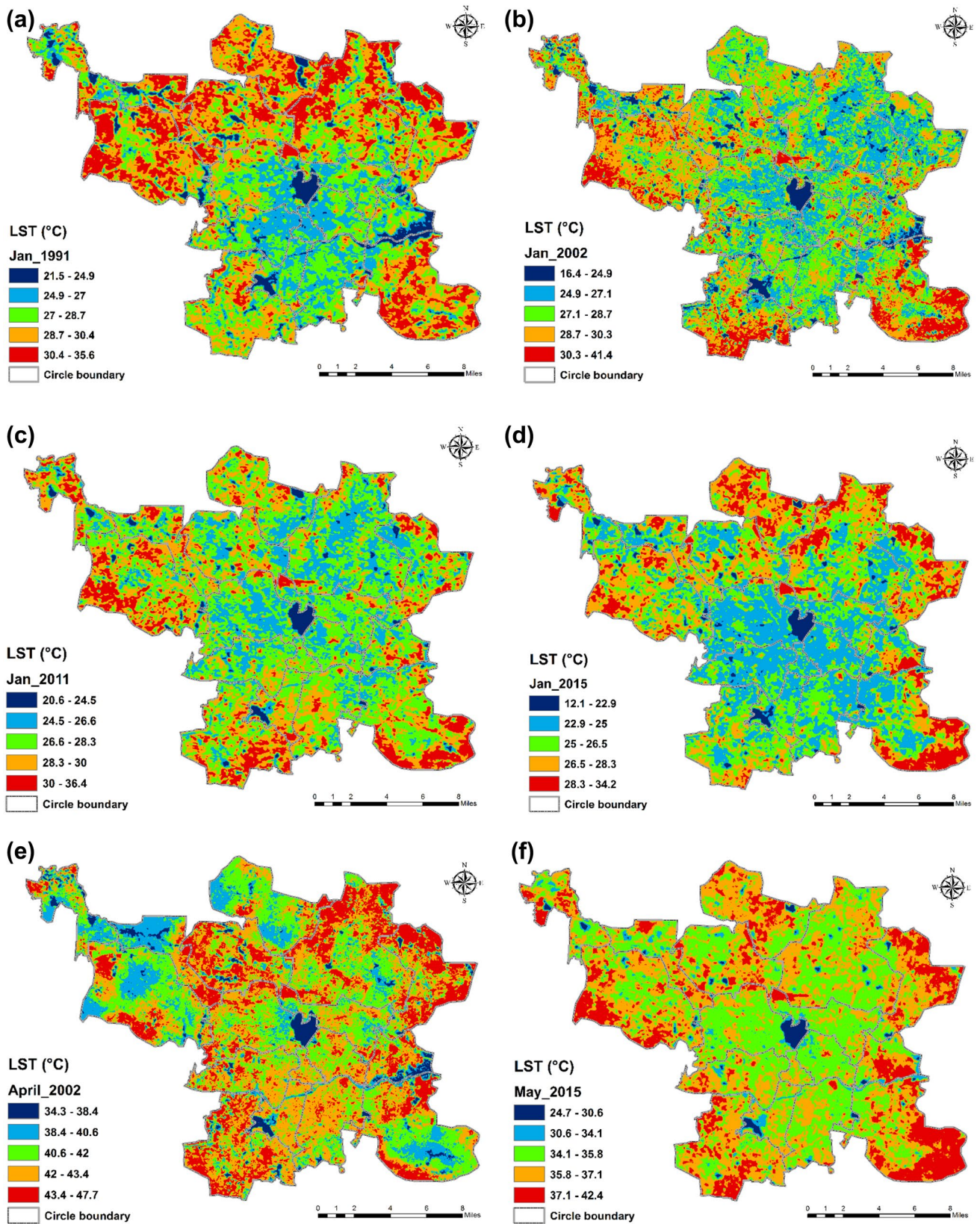


Fig. 7 Spatio-temporal variation of land surface temperature (LST) on **a** 27th Jan 1991, **b** 17th Jan 2002, **c** 18th Jan 2011, **d** 13th Jan 2015, **e** 7th April 2002, **f** 21st May 2015, **g** 14th September 2002, **h** 1st October 2011, **i** 12th October 2015 in the study area

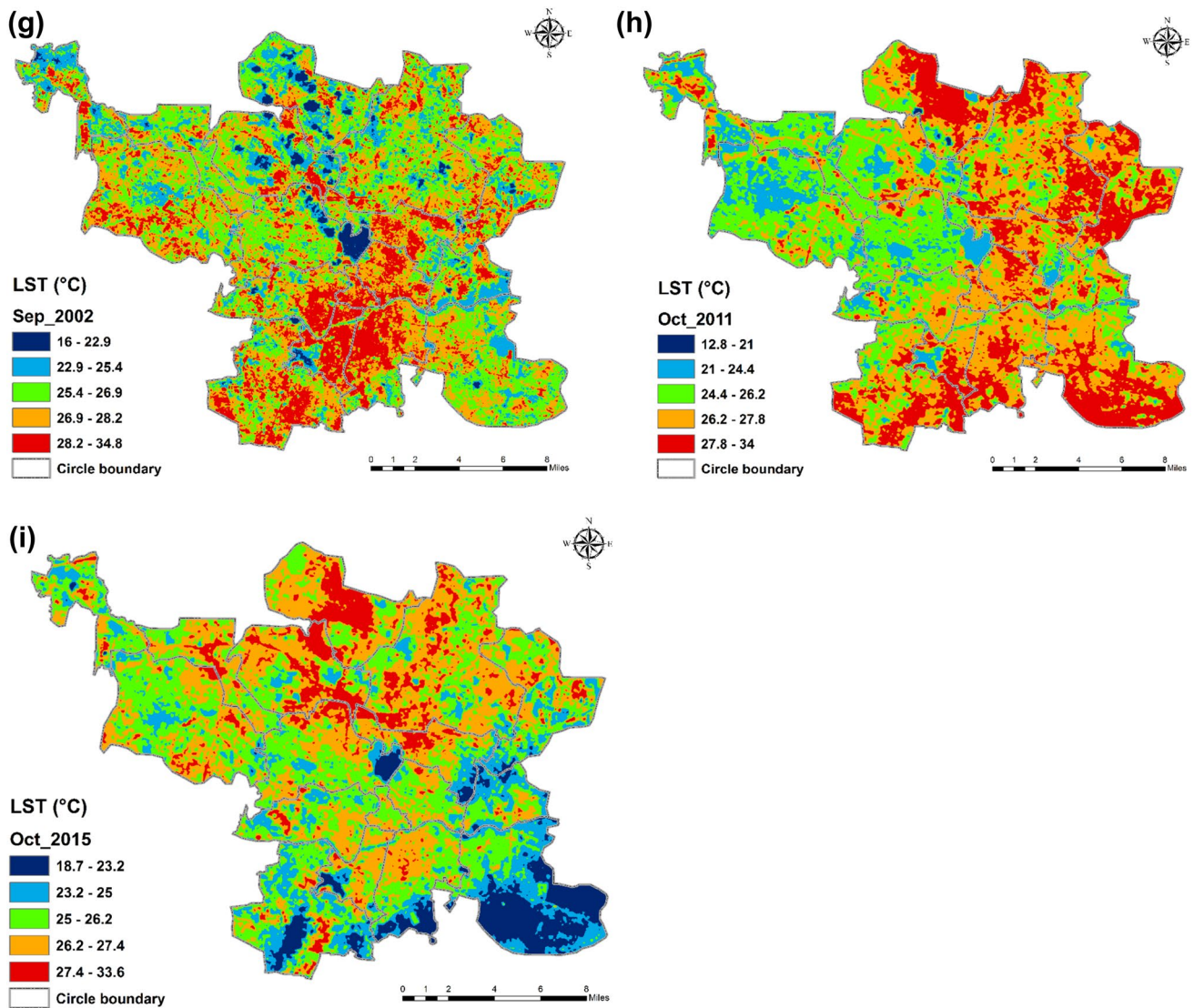


Fig. 7 (continued)

the incremental LST for all indices, followed by farmland, urban built-up, urban green space and aquatic vegetation class, respectively.

Discussion

Correlation between urban biophysical composition and LST and UHI

As it can be seen in Fig. 10, the spatial coherence between NDVI, LSWI, NDBaI and NDBI was found very high over the areas occupied by the built-up urban surface, which substantially indicates the importance of surface moisture content, amount, and nature of vegetation cover and thermal properties of soil on surface energy exchanges (Deng

and Wu 2013c). Also, the high negative correlation between LST and biophysical composition observed across the city exhibits the physical significance of vegetation to moderate UHI and LST (Weng et al. 2004). Though the sensitivity and degree of association between LST and biophysical composition varied among different LULC (Fig. 14; Table 1). The similar has been reported earlier, where the presence of UHI cluster within the city controlled by the surface moisture content, fraction of vegetation cover, impervious fraction to a larger extent (Guo et al. 2015). Moreover, irrespective of LULC, Guo et al. 2015 have been found that both NDVI (negatively) and NDBaI (positively) are significantly correlated with LST and UHI. However, in our study, we observed that, among the five major LULC classes, NDBaI mitigates the UHI and LST over aquatic vegetation and green space cover areas, whereas, the rest

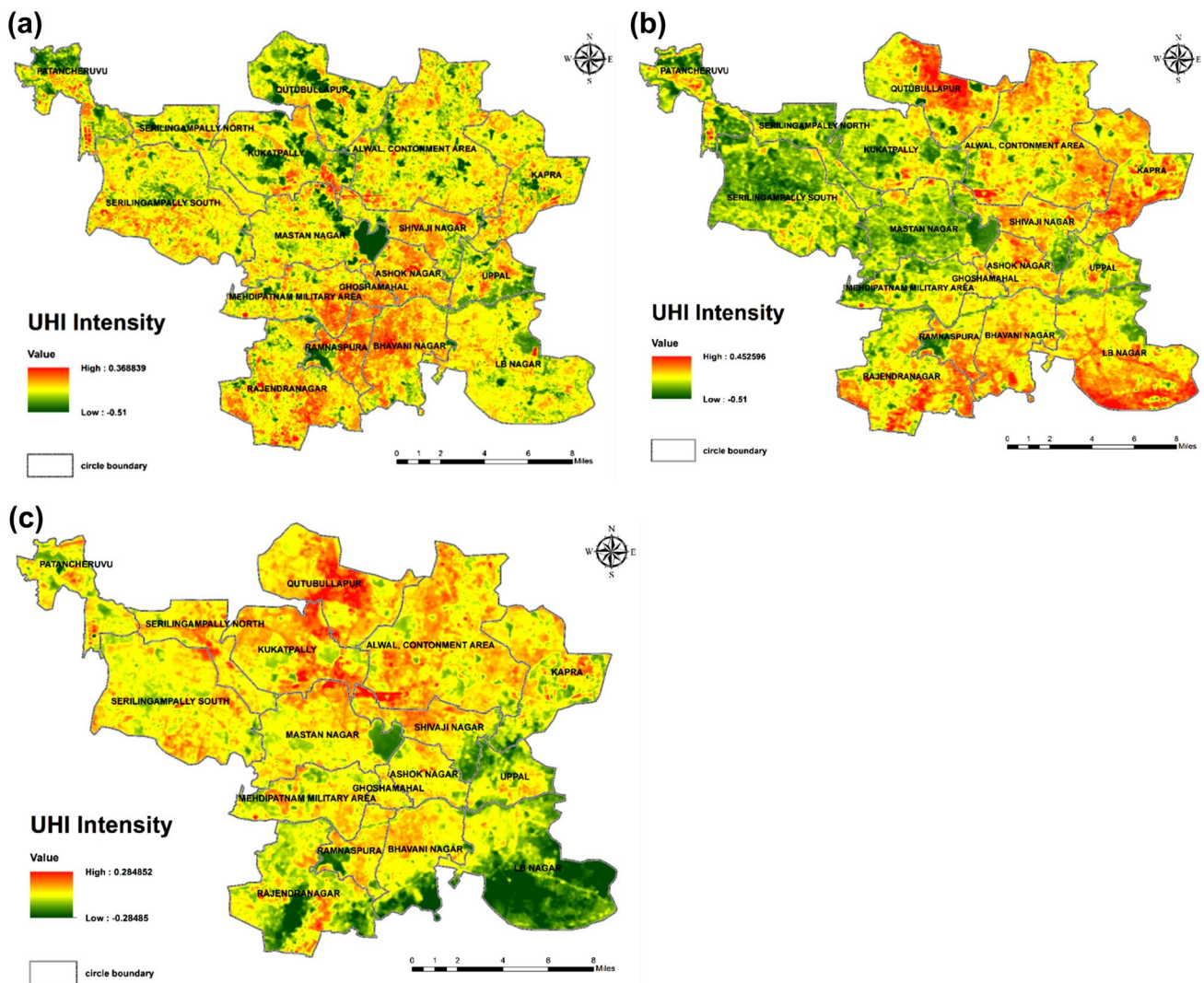


Fig. 8 Shows the nature of Urban Heat Island (UHI) Intensity on **a** September 2002, **b** October 2011 and **c** October 2015 in GHMC

three LULC classes were strengthening the UHI. This nonlinearly can be attributed due to the high variability of surface moisture dynamics across the study region. As it has been reported by Deng and Wu 2013c, land class with very low NDVI values could be composed by a variety of non-vegetated components, i.e. dark and bright impervious soil made of concrete basalts, dark and moist soil with high organic matter content etc. which is very difficult to be characterized only by NDVI and having distinct reflectance properties within the thermal spectrum (Yuan and Bauer 2007; Li et al. 2011; Deng and Wu 2013c). In this study, the correlation between NDVI and estimated LST ranged from $R^2=0.6-0.7$, similar to the $R^2=0.49$ (Yue et al. 2007), $r=0.67$ (Guo et al. 2015), $r=0.69$ (Zhu et al. 2013), $R^2=0.83$ (Li et al. 2011). While, the NDBI ($r \geq 0.8$) and NDBaI ($r \geq 0.6$) were being found to strengthen the UHI mostly, also been observed by Deng and Wu (2013c) using

physical spectral unmixing and thermal mixing (SUTM) model depicts that in urban areas, NDBI and NDBaI based impervious fraction performs consistently and explained maximum variances than that of less impervious (rural) areas.

The correlation between vegetation and moisture abundance of each LULC and LST was examined using Pearson correlation coefficient test and regression analysis (Table 1) with 0.05 and 0.01 significance level. It can be seen in Table 1, which shows LST was negatively correlated with NDVI for all LULC classes with a different intensity. The highest negative association between NDVI and LULC types were accounted over the areas occupied by aquatic vegetation class ($r = -0.86$), followed by urban green space ($r = 0.82$), urban built-up ($r = -0.8$), farmland ($r = -0.58$) and follow land ($r = -0.52$), results is similar with the Indianapolis, USA (Weng et al. 2004), whereas,

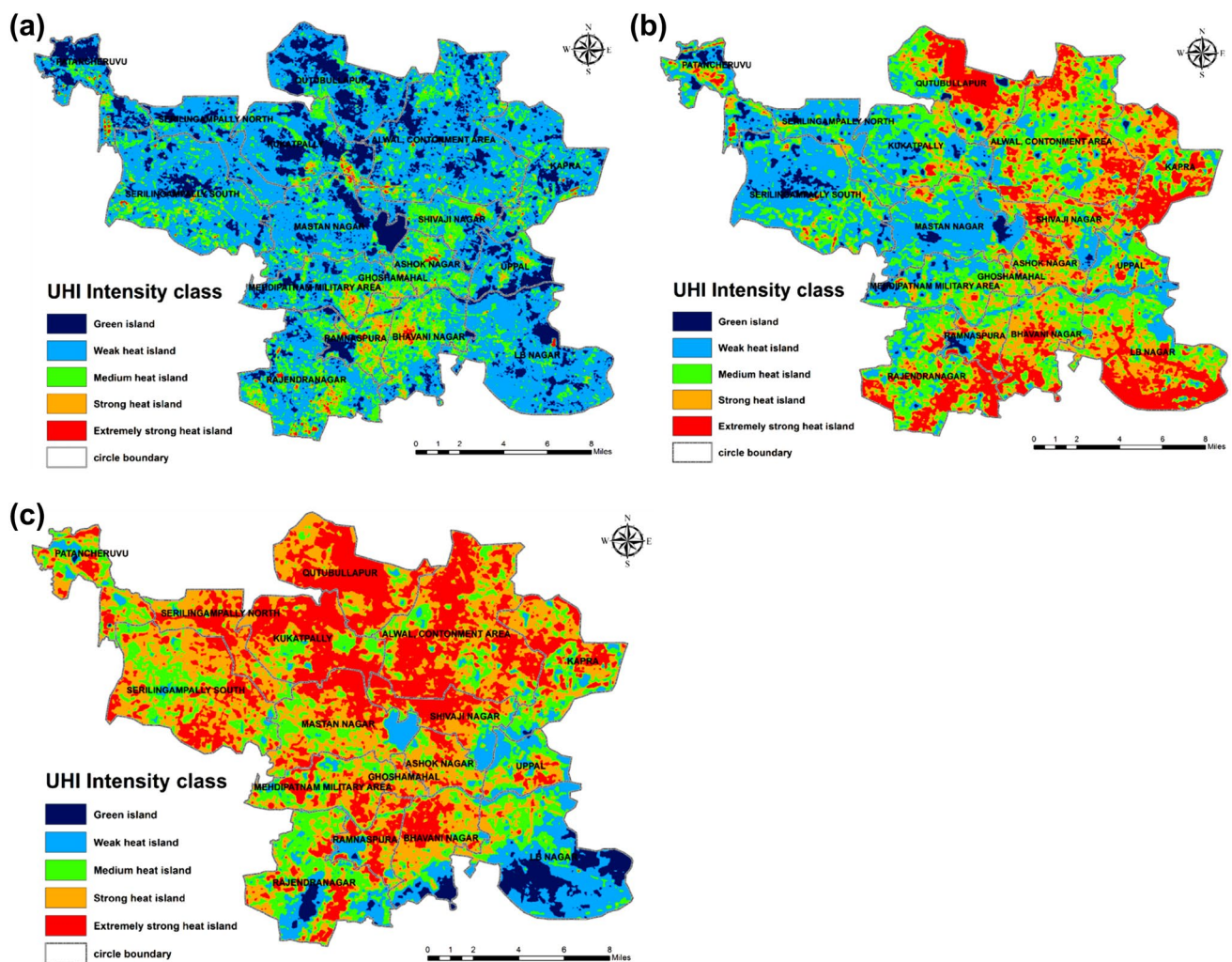


Fig. 9 Spatial distribution of UHI intensity classes in GHMC observed in **a** 2002, **b** 2011 and **c** 2015

maximum negative correlation between NDVI and LST at 30 m resolution scale was found in cropland ($r = -0.73$), forest ($r = -0.72$), urban built-up ($r = -0.62$) and grassland ($r = -0.36$), respectively. Concerning the coherence between LSWI and LST, the highest values has been observed in built-up urban areas ($r = -0.84$), followed by aquatic vegetation cover ($r = -0.83$), fallow land ($r = -0.82$), farmland ($r = -0.78$) and urban green spaces ($r = -0.75$), respectively. It is worth to notice that, among all indices, NDBI explain the maximum model variance with the highest correlation value ($r = 0.84$), followed by LSWI ($r = -0.8$), NDBaI ($r = 0.79$) and NDVI ($r = -0.7$) for all LULC types strongly indicates the impact of surface imperviousness on thermal anomalies and surface energy balance of a city region.

LULC dynamics and its impact on surface UHI and LST

The spatiotemporal distribution and changes of different LULC categories since 1973 to 2015 are shown in Fig. 2. It can be seen in Fig. 4, that the estimated LST has been varied distinctly over the central built-up urban areas in comparison to other classes. This is an indication of the presence of hot objects especially in the central part of the region displaying the more importance of influencing surface UHI patterns (Weng et al. 2007). The similar has been observed while built-up impervious surface (hot objects) was found positively correlated with LST and vegetation (cold objects) was negatively associated with LST ensembles the impact of thermal fractional components (hot objects and cold objects) in conjunction with the biophysical descriptors (NDVI, LSWI, NDBI, NDBaI) to changes

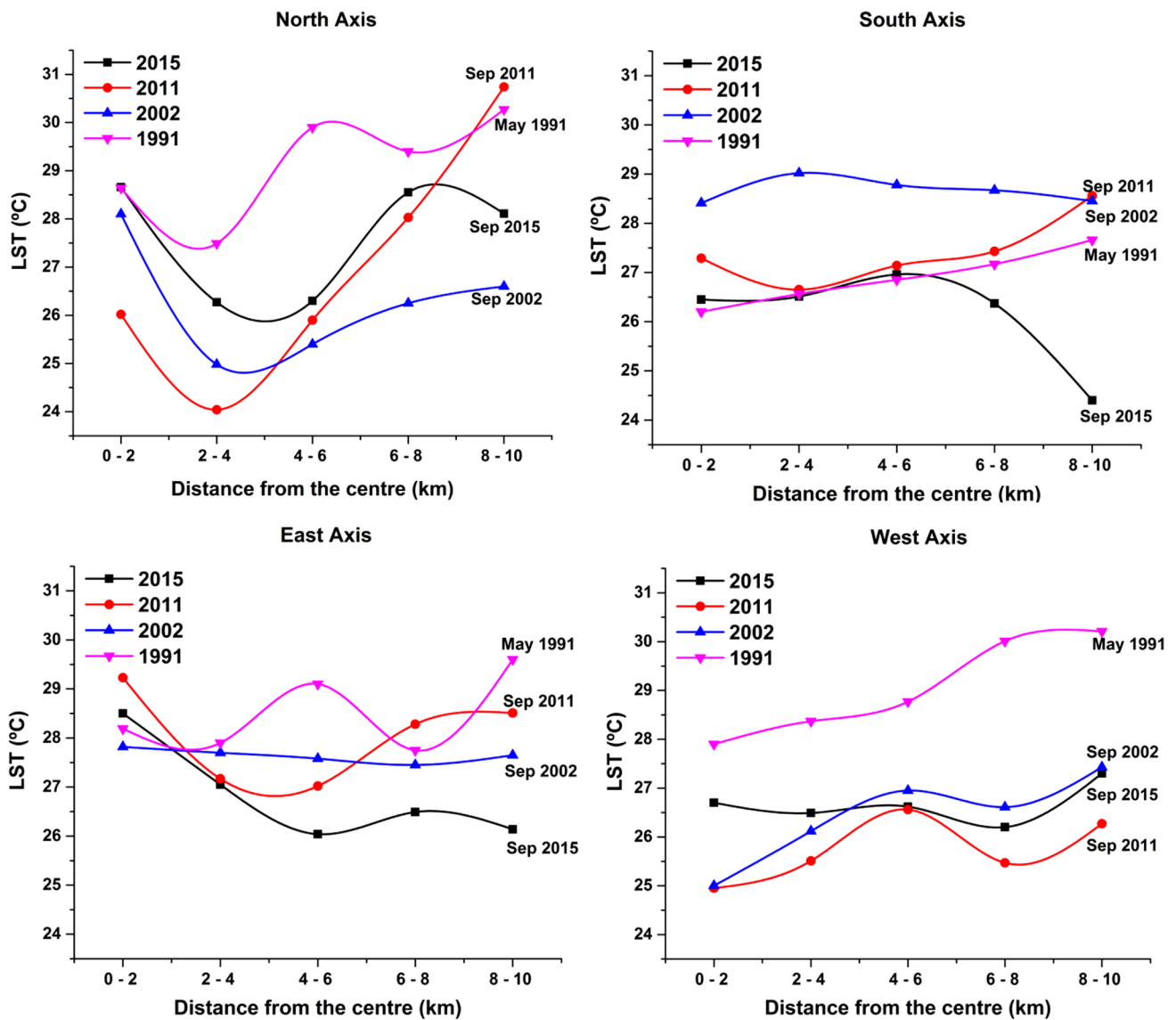


Fig. 10 LST retrieved from four transects having 2 km interval from the urban hotspot cluster for 1991, 2002, 2011 and 2015, respectively

Table 2 Changes of LST (°C) in different LULC classes from 2002 to 2015

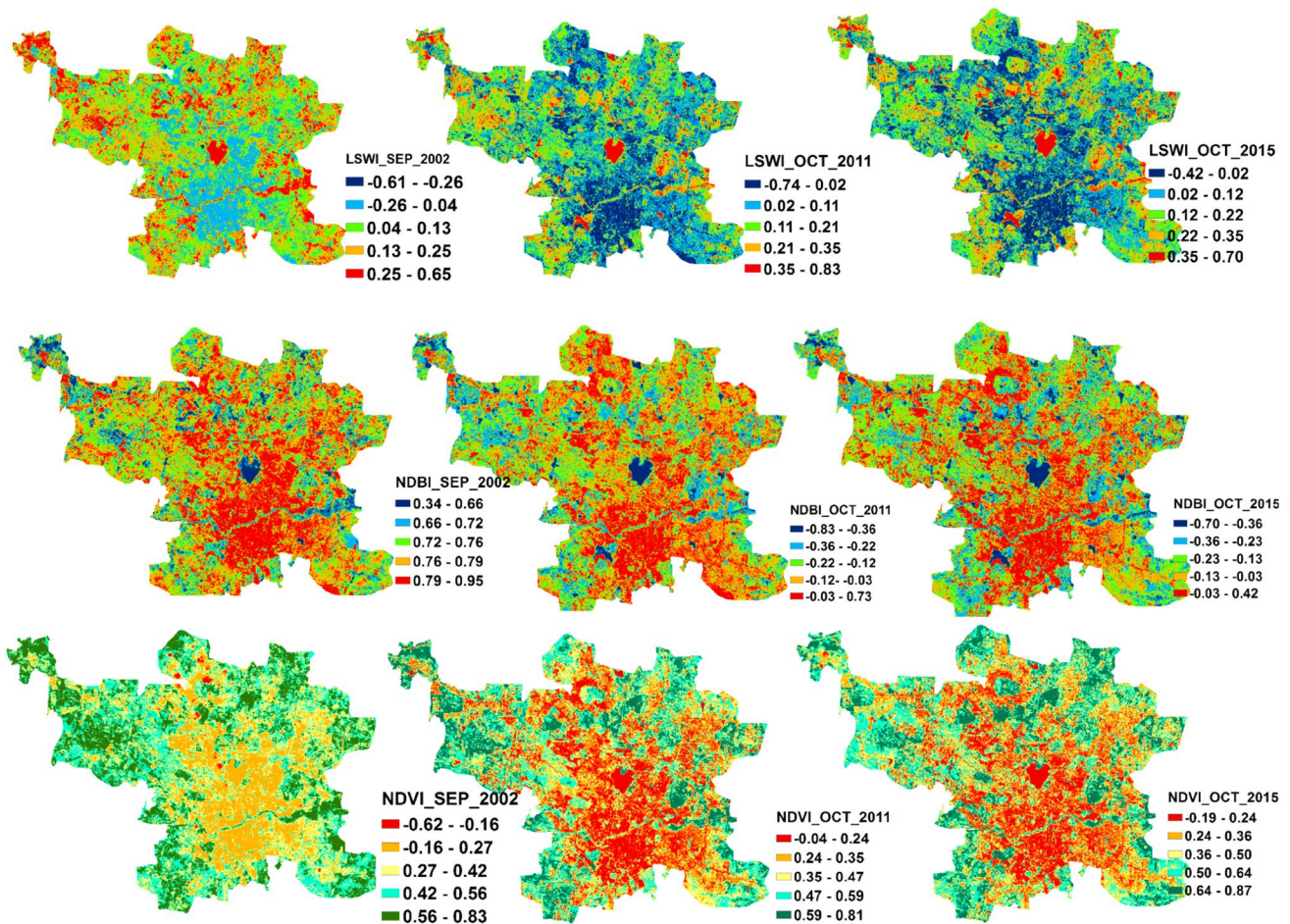
LULC	2002				2011				2015			
	Min	Max	Mean	Range	Min	Max	Mean	Range	Min	Max	Mean	Range
A. vegetation	16.3	34.3	25.3	18	15.6	32.9	24.3	17.3	19.1	31.2	25.2	12.1
Water body	18.9	28.3	23.6	9.4	21.9	29.1	25.5	7.2	18.9	26.8	22.9	7.9
Built up land	16.1	34.8	25.5	18.7	12.8	33.2	23	20.4	18.7	33.6	26.2	14.9
Farm land	17.1	33.1	25.1	16	17.9	34.1	26	16.2	19.7	30.9	25.3	11.2
Fallow land	16.5	33.5	25	17	17.5	32.3	24.9	14.8	19.4	31.8	25.8	12.44
Green space	16.6	32.9	24.8	16.3	17.5	34	25.8	16.5	19	33.4	26.2	14.4

the spatiotemporal pattern of LST cluster in a city (Lu and Weng 2006). However, the uses of the biophysical descriptor, especially NDVI to examine the SUHI phenomenon are suggested to restrict for all season as NDVI suffers from

apparent seasonal variation (Yuan and Bauer 2007). The changing dynamics of different UHI classes from 2002 to 2015 are shown in Table 2. The maximum pace of changes among the UHI classes had seen in the extremely strong

Table 3 Spatiotemporal UHI class dynamics during 2002 to 2015 in Hyderabad city

UHI class	2002		2015		Change during 2002–2015	
	Area	% of area	Area	% of area	Area	Rate of changes
Green island	108.58	16.27	10.58	1.58	−98.00	−6.94
Weak heat island	402.23	60.27	138.58	20.77	−263.66	−5.04
Medium heat island	126.40	18.94	321.02	48.10	194.62	11.84
Strong heat island	26.32	3.94	157.37	23.58	131.05	38.30
Extremely strong heat island	3.83	0.57	39.75	5.96	35.92	72.22
	667.37	100.00	667.37	100.00		

**Fig. 11** Spatiotemporal changes of LSWI, NDBI, and NDVI on Sep 2002, Oct 2011 and 2015 in the study region

urban heat island categories (72.22), followed by strong heat island (38.3), medium heat island (11.84), weak heat island (−5.04) and green island (−6.94), respectively. It can also be noted that built-up urban area was the dominant land use types in extremely heat island zones, whereas, vegetation and water bodies characterize the green island and weak heat island areas. The similar has been observed Liu and Weng 2008, where the spatial configuration of dominant LULC types are controlling the spatial configuration of the different temperature and UHI clusters in that

zone. The temperature and vegetation index (TVX) space was used in several studies to examine the individual and multiplicative impact of different LULC types on LST and UHI dynamics (Lambin and Ehrlich 1996, 1997; Gillies et al. 1997; Sandholt et al. 2002; Goward et al. 2002). The spatial distribution and temporal dynamics of different UHI classes for the year of 2002, 2011 and 2015 are shown in Fig. 6. This could be attributed to the discrepant nature of surface LST across the city region with uneven spatial expansion of extremely strong and strong heat island at the

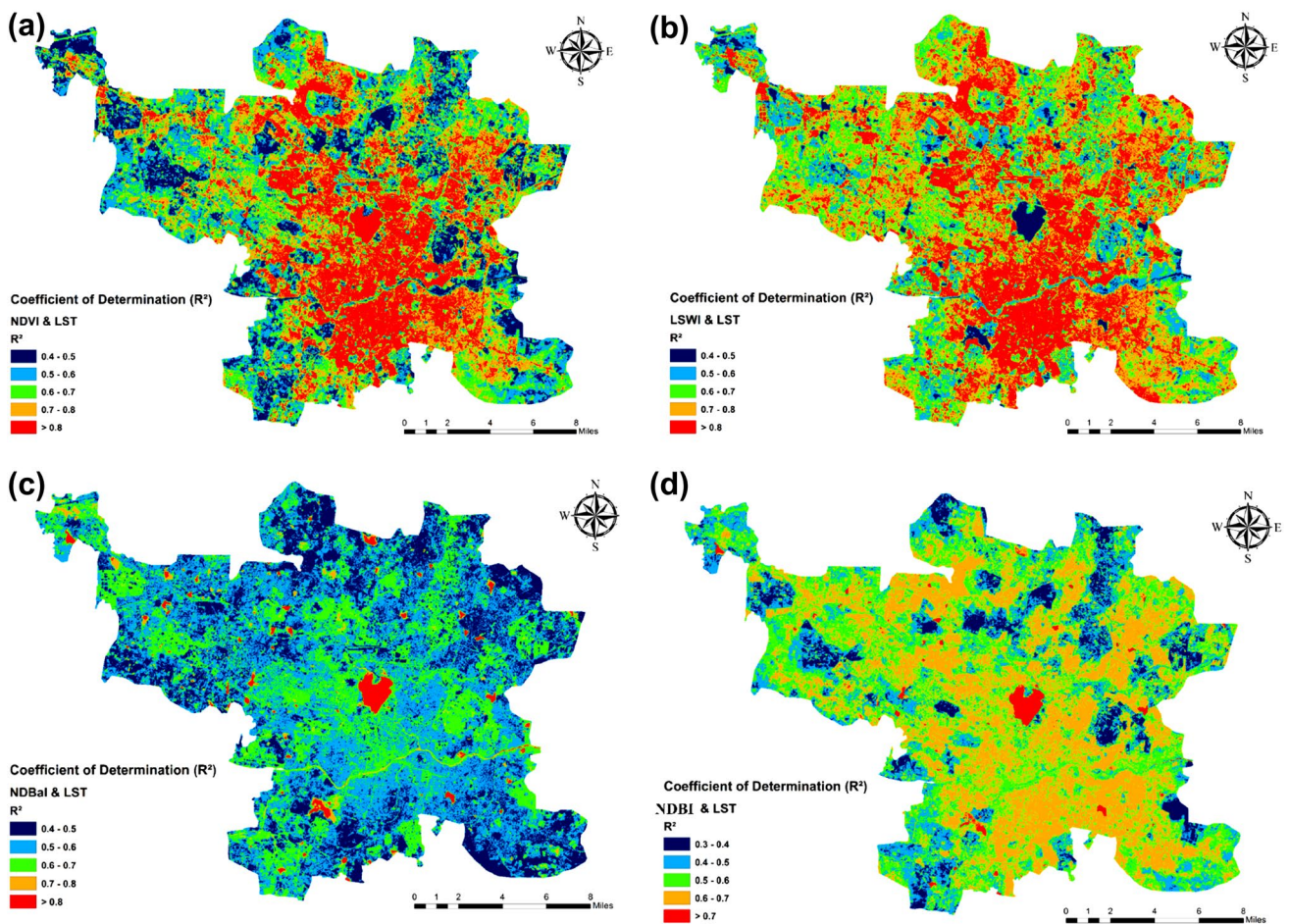


Fig. 12 Shows the spatial coherence between the biophysical indices; i.e. **a** NDVI, **b** LSWI, **c** NDBaI and **d** NDBI and LST

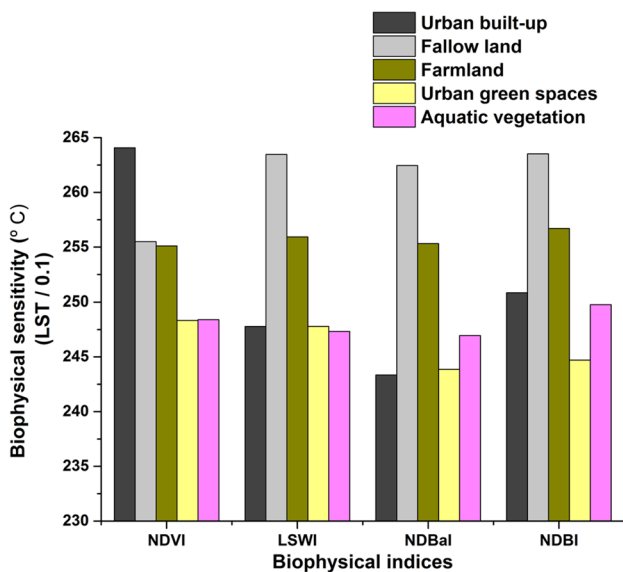


Fig. 13 Shows the sensitivity between LST and the biophysical variables (NDVI, LSWI, NDBaI and NDBI) in different LULC categories across the study region

expense of natural and semi-natural surface cover leads to undesirable thermal anomalies in GHMC due to uncontrolled urban expansion. The similar has been observed in PRD, in Guangdong Province, southern China, is one of the regions experiencing rapid urbanization that has resulted in remarkable UHI effect, which is affecting the regional climate, environment, and socio-economic development to a larger extent (Chen et al. 2006). However, the estimated LST being varied highly in intra LULC classes than that of inter LULC variation. The biophysical sensitivity between the indices and LST for different LULC was assessed in this study and are drawn in Fig. 12. In built-up urban areas, NDVI is found highly sensitive with LST, followed by NDBI, LSWI, and NDBaI, respectively, indicates the cumulative importance of urban green cover to moderate UHI and thermal discomfort of a city. However, fallow land shows the same sensitivity for LSWI, NDBI, and NDBaI, and less sensitivity between NDVI and LST exhibited the less green coverage in this zone. Farmland is being found less sensitive with LST, followed by aquatic vegetation cover and urban green cover, respectively.

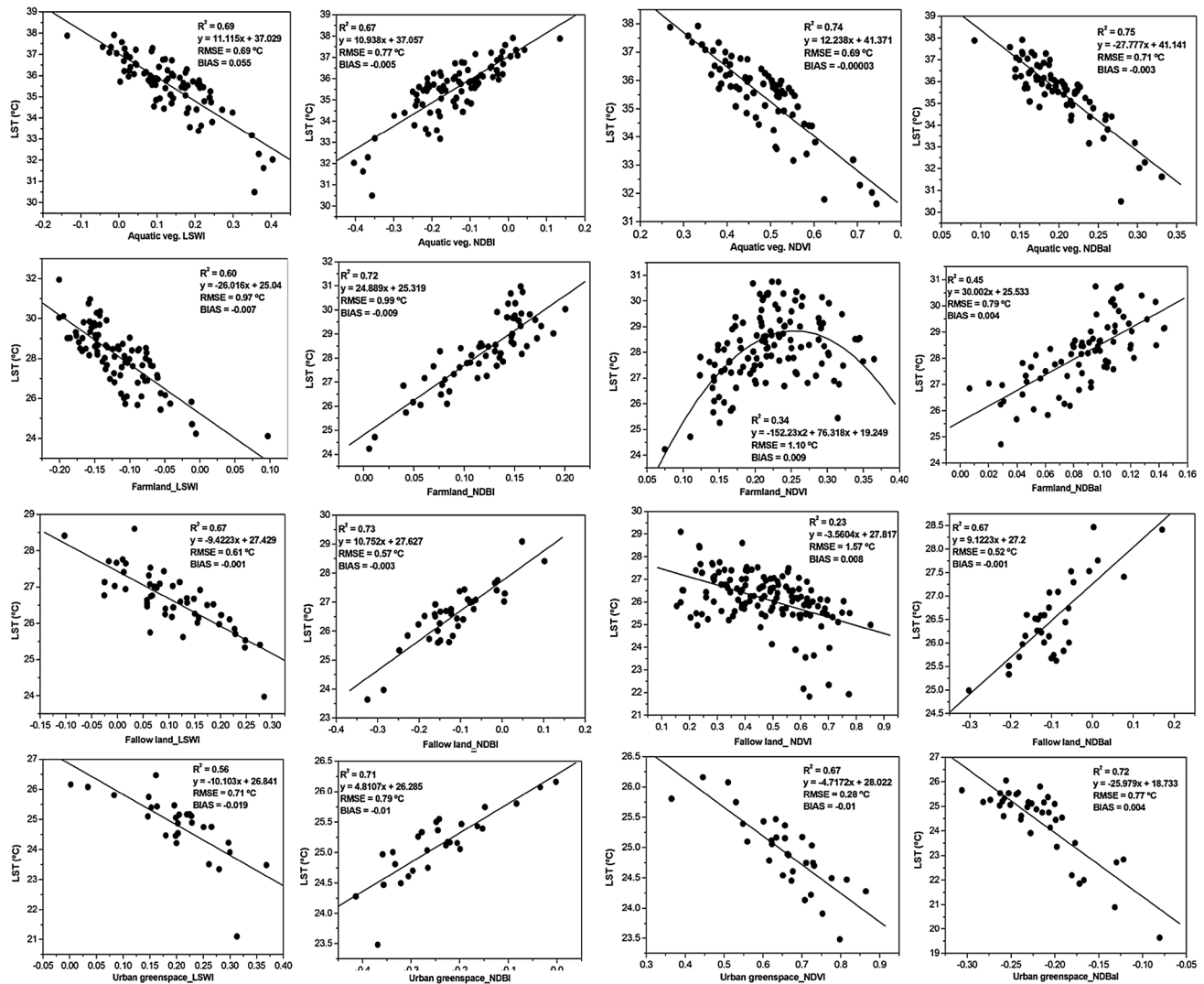


Fig. 14 shows the coherence between LST and biophysical indices (LSWI, NDBI, NDVI, and NDBaI) for four different LULC categories, viz. aquatic vegetation, farmland, fallow land and urban built-up, respectively

Conclusion

In this study, the discrepant effects of urbanization and biophysical changes on UHI have been investigated in Hyderabad city, the sixth largest urban agglomeration of India. The spatially explicit coherence between the selected indices and UHI of different LULC classes are found highly correlated across the region. Therefore, the main conclusions of the study are as follows: (1) LST was negatively correlated with NDVI for all LULC classes with a different intensity. The highest negative association between NDVI and LULC types were accounted over the areas occupied by aquatic vegetation class ($r = -0.86$), followed by urban green space ($r = 0.82$), urban built-up ($r = -0.8$), farmland ($r = -0.58$) and follow land ($r = -0.52$), respectively. (2) Among all indices, NDBI explain the maximum model

variance with the highest correlation value ($r = 0.84$), followed by LSWI ($r = -0.8$), NDBaI ($r = 0.79$) and NDVI ($r = -0.7$) for all LULC types strongly indicates the impact of surface imperviousness on thermal anomalies and surface energy balance of a city region. (3) Among the five major LULC classes, NDBaI mitigates the UHI and LST over aquatic vegetation and green surface areas, whereas, the rest three LULC classes were strengthening the UHI. (4) The biophysical sensitivity between the indices and LST for different LULC were varied distinctly. In built-up urban areas, NDVI is found highly sensitive with LST, followed by NDBI, LSWI, and NDBaI. (5) Among the five UHI classes, extremely strong urban heat island categories changes rapidly (72.22) during 2002–2015, followed by strong heat island (38.3), medium heat island (11.84), weak heat island (-5.04) and green island (-6.94), respectively.

Table 4 Biophysical dynamics of different LULC and its relationship with LST (°C) in Hyderabad city

LULC	Linear model	R^2	r	RMSE (°C)	Bias	σ	P
Aquatic vegetation							
NDVI and LST	$y = 12.238x + 41.371$	0.74	-0.86	0.69	0.005	1.36	<0.01
LSWI and LST	$y = -11.115x + 37.029$	0.69	-0.83	0.75	0.055	1.33	<0.01
NDBaI and LST	$y = -27.777x + 41.141$	0.75	-0.87	0.72	-0.003	1.44	<0.01
NDBI and LST	$y = 10.938x + 37.057$	0.67	0.82	0.77	-0.005	1.35	<0.01
Urban green spaces							
NDVI and LST	$y = -4.7172x + 28.022$	0.67	-0.82	0.28	0.074	0.50	<0.01
LSWI and LST	$y = -10.103x + 26.841$	0.56	-0.75	0.71	-0.02	1.07	<0.01
NDBaI and LST	$y = -25.979x + 18.733$	0.72	-0.85	0.78	0.005	1.47	<0.01
NDBI and LST	$y = 4.8107x + 26.285$	0.71	0.84	0.79	-0.01	1.50	<0.01
Farmland							
NDVI and LST	$y = -152.23x^2 + 76.318x + 19.249$	0.34	-0.58	1.11	0.01	1.36	<0.05
LSWI and LST	$y = -26.016x + 25.04$	0.61	-0.78	0.98	-0.01	1.54	<0.01
NDBaI and LST	$y = 30.002x + 25.533$	0.45	0.67	1.00	0.04	1.34	<0.01
NDBI and LST	$y = 24.889x + 25.319$	0.72	0.85	0.76	-0.01	1.44	<0.01
Fallow land							
NDVI and LST	$y = -7.7439x^2 + 3.6982x + 26.308$	0.27	-0.52	1.56	0.01	1.78	<0.05
LSWI and LST	$y = -9.4223x + 27.429$	0.67	-0.82	0.61	0.001	1.01	<0.01
NDBaI and LST	$y = 9.1223x + 27.2$	0.68	0.83	0.53	-0.001	0.92	<0.01
NDBI and LST	$y = 10.752x + 27.627$	0.73	0.85	0.57	-0.003	1.10	<0.01
Urban built-up							
NDVI and LST	$y = -8.0082x + 28.027$	0.65	-0.80	0.68	-0.001	1.16	<0.01
LSWI and LST	$y = -17.664x + 25.849$	0.71	-0.84	1.01	0.01	1.88	<0.01
NDBaI and LST	$y = -25.623x + 21.02$	0.59	0.77	1.10	0.03	1.73	<0.01
NDBI and LST	$y = 17.453x + 26.34$	0.73	0.85	1.03	0.02	1.99	<0.01

(6) The high negative correlation between LST and biophysical composition observed across the city exhibits the physical significance of vegetation to moderate UHI and LST.

Acknowledgements SS acknowledges UGC for providing continuous research fellowship to carry out the research at Indian Institute of Technology (IIT), Kharagpur (India). SB would like to acknowledge INSPIRE Fellowship Programme (Award Number: IF131138) funded by Department of Science and Technology (DST, New Delhi) for doctoral research being carried out at the Indian Institute of Technology (IIT), Kharagpur (India). SR thanks the Ministry of Human Resource Development (MHRD, New Delhi) for providing continuous research fellowship for doctoral work being carried out at the Indian Institute of Technology (IIT), Kharagpur (India). SS and SR appreciates the support and encouragement got from Prof. Somnath Sen, Prof. Saitkat Kumar Paul and Prof. Joy Sen, Indian Institute of Technology Kharagpur (India) and, SB are thankful to Prof. M. A. Mamtani, Indian Institute of Technology Kharagpur (India).

References

Amiri R, Weng Q, Alimohammadi A, Alavipanah SK (2009) Spatial-temporal dynamics of land surface temperature in relation

to fractional vegetation cover and land use/cover in the Tabriz urban area, Iran. *Remote Sens Environ* 113(12):2606–2617. doi:10.1016/j.rse.2009.07.021

Arvidson T (2002) Personal Correspondence, Landsat-7 Senior Systems Engineer, Landsat Project Science Office, Goddard Space Flight Center, Washington, D.C

Ayanlade A (2016) Variation in diurnal and seasonal urban land surface temperature: landuse change impacts assessment over Lagos metropolitan city. *Model Earth Systems Environ* 2(4):1–8. doi:10.1007/s40808-016-0238-z

Barsi JA, Schott JR, Palluconi FD, Helder DL, Hook SJ, Markham BL et al (2003) Landsat TM and ETM + thermal band calibration. *Can J Remote Sens* 29(2):141–153

Bottayaa Z, Unger J (2003) A multiple linear statistical model for estimating the mean maximum urban heat island. *Theor Appl Climatol* 75(3–4):233–243. Doi:10.1007/S00704-003-0735-7

Buyantuyev A, Wu J (2010) Urban heat islands and landscape heterogeneity: linking spatiotemporal variations in surface temperatures to land-cover and socioeconomic patterns. *Landsc Ecol* 25(1):17–33. doi:10.1007/s10980-009-9402-4

Cao X, Onishi A, Chen J, Imura H (2010) Quantifying the cool island intensity of urban parks using ASTER and IKONOS data. *Landsc Urban Plan* 96(4):224–231. doi:10.1016/j.landurbplan.2010.03.008

Carlson TN, Ripley DA (1997) On the relation between NDVI, fractional vegetation cover, and leaf area index. *Remote Sens Environ* 62(3):241–252. doi:10.1016/S0034-4257(97)00104-1

- Carlson TN, Traci Arthur S (2000) The impact of land use—land cover changes due to urbanization on surface microclimate and hydrology: a satellite perspective. *Glob Planet Change* 25(1–2):49–65. Doi:[10.1016/S0921-8181\(00\)00021-7](https://doi.org/10.1016/S0921-8181(00)00021-7)
- Carlson TN, Gillies RR, Perry EM (1994) A method to make use of thermal infrared temperature and NDVI measurements to infer surface soil water content and fractional vegetation cover. *Remote Sens Rev* 9:161–173
- Chander G, Markham B (2003) Revised landsat-5 TM radiometric calibration procedures and postcalibration dynamic ranges. *IEEE Trans Geosci Remote Sens* 41(11 PART II):2674–2677. doi:[10.1109/TGRS.2003.818464](https://doi.org/10.1109/TGRS.2003.818464)
- Chander G, Markham BL, Helder DL (2009) Summary of current radiometric calibration coefficients for Landsat MSS, TM, ETM+, and EO-1 ALI sensors. *Remote Sens Environ* 113(5):893–903. doi:[10.1016/j.rse.2009.01.007](https://doi.org/10.1016/j.rse.2009.01.007)
- Chen XL, Zhao HM, Li PX, Yin ZY (2006) Remote sensing image-based analysis of the relationship between urban heat island and land use/cover changes. *Remote Sens Environ* 104(2):133–146. doi:[10.1016/j.rse.2005.11.016](https://doi.org/10.1016/j.rse.2005.11.016)
- Chudnovsky A, Ben-Dor E, Saaroni H (2004) Diurnal thermal behavior of selected urban objects using remote sensing measurements. *Energy Build* 36(11):1063–1074. doi:[10.1016/j.enbuild.2004.01.052](https://doi.org/10.1016/j.enbuild.2004.01.052)
- Chun B, Guldmann J-M (2014) Spatial statistical analysis and simulation of the urban heat island in high-density central cities. *Landsc Urban Plan* 125:76–88. doi:[10.1016/j.landurbplan.2014.01.016](https://doi.org/10.1016/j.landurbplan.2014.01.016)
- Deng C, Wu C (2013a) A spatially adaptive spectral mixture analysis for mapping subpixel urban impervious surface distribution. *Remote Sens Environ* 133:62–70. doi:[10.1016/j.rse.2013.02.005](https://doi.org/10.1016/j.rse.2013.02.005)
- Deng C, Wu C (2013b) Estimating very high resolution urban surface temperature using a spectral unmixing and thermal mixing approach. *Int J Appl Earth Obs Geoinf* 23(1):155–164. doi:[10.1016/j.jag.2013.01.001](https://doi.org/10.1016/j.jag.2013.01.001)
- Deng C, Wu C (2013c) Examining the impacts of urban biophysical compositions on surface urban heat island: a spectral unmixing and thermal mixing approach. *Remote Sens Environ* 131:262–274. doi:[10.1016/j.rse.2012.12.020](https://doi.org/10.1016/j.rse.2012.12.020)
- Feddema JJ, Oleson KW, Bonan GB, Mearns LO, Buja LE, Meehl GA, Washington WM (2005) The importance of land-cover change in simulating future climates. *Science* 310(5754):1674–1678. doi:[10.1126/science.1118160](https://doi.org/10.1126/science.1118160)
- Foley AJ, Defries R, Asner GP, Barford C, Bonan G, Carpenter SR, Snyder PK (2005) Global consequences of land use. *Science* 309(5734):570–574. doi:[10.1126/science.1111772](https://doi.org/10.1126/science.1111772)
- Gillies RR, Kustas WP, Humes KS (1997) A verification of the “triangle” method for obtaining surface soil water content and energy fluxes from remote measurements of the normalized difference vegetation index (NDVI) and surface ϵ . *Int J Remote Sens* 18(15):3145–3166. Doi:[10.1080/014311697217026](https://doi.org/10.1080/014311697217026)
- Goward SN, Xue Y, Czajkowski KP (2002) Evaluating land surface moisture conditions from the remotely sensed temperature/vegetation index measurements: an exploration with the simplified simple biosphere model. *Remote Sens Environ* 79(2–3):225–242
- Guo G, Wu Z, Xiao R, Chen Y, Liu X, Zhang X (2015) Impacts of urban biophysical composition on land surface temperature in urban heat island clusters. *Landsc Urban Plan* 135:1–10. doi:[10.1016/j.landurbplan.2014.11.007](https://doi.org/10.1016/j.landurbplan.2014.11.007)
- He C, Shi P, Xie D, Zhao Y (2010) Improving the normalized difference built-up index to map urban built-up areas using a semi-automatic segmentation approach. *Remote Sens Lett* 1(4):213–221. doi:[10.1080/01431161.2010.481681](https://doi.org/10.1080/01431161.2010.481681)
- Ishola AK, Okogbue EC, Adeyeri OE (2016) Dynamics of surface urban biophysical compositions and its impact on land surface thermal field. *Model Earth Syst Environ* 0(4):1–20. doi:[10.1007/s40808-016-0265-9](https://doi.org/10.1007/s40808-016-0265-9)
- Jackson TJ, Chen D, Cosh M, Li F, Anderson M, Walthall C, Doriaswamy P, Hunt ER (2004) Vegetation water content mapping using Landsat data derived normalized difference water index for corn and soybeans. *Remote Sens Environ* 92:475–482
- Kalnay E, Cai M (2003) Impact of urbanization and land use on climate change. *Nature* 423:528–531
- Kayet N, Pathak K, Chakrabarty A, Sahoo S (2016) Spatial impact of land use/land cover change on surface temperature distribution in Saranda Forest, Jharkhand. *Model Earth Syst Environ* 2(3):1–10. doi:[10.1007/s40808-016-0159-x](https://doi.org/10.1007/s40808-016-0159-x)
- Lambin FF, Ehrlich D (1996) The surface temperature–vegetation index space for land use and land cover change analysis. *Int J Remote Sens* 17:463–487
- Lambin EF, Ehrlich D (1997) Land-cover changes in Sub-Saharan Africa (1982–1991): application of a change index based on remotely sensed surface temperature and vegetation indices at a continental scale. *Remote Sens Environ* 61(2):181–200. Doi:[10.1016/S0034-4257\(97\)00001-1](https://doi.org/10.1016/S0034-4257(97)00001-1)
- Landsberg HE (1981) *The Urban climate*. Academic, New York
- Li J, Song C, Cao L, Zhu F, Meng X, Wu J (2011) Impacts of landscape structure on surface urban heat islands: a case study of Shanghai, China. *Remote Sens Environ* 115(12):3249–3263. doi:[10.1016/j.rse.2011.07.008](https://doi.org/10.1016/j.rse.2011.07.008)
- Liu H, Weng Q (2008) Seasonal variations in the relationship between landscape pattern and land surface temperature in Indianapolis, USA. *Environ Monit Assess* 144(1–3):199–219. doi:[10.1007/s10661-007-9979-5](https://doi.org/10.1007/s10661-007-9979-5)
- Lu D, Weng Q (2006) Use of impervious surface in urban land-use classification. *Remote Sens Environ* 102(1–2):146–160. doi:[10.1016/j.rse.2006.02.010](https://doi.org/10.1016/j.rse.2006.02.010)
- Maki M, Ishihara M, Tamura M (2004) Estimation of leaf water status to monitor the risk of forest fires by using remotely sensed data. *Remote Sens Environ* 90:441–450
- Markham BL, Barker JL (1985) Spectral characterization of the LANDSAT Thematic Mapper sensors’. *Int J Remote Sens* 6(5):697–716
- Oke TR (1987) *Boundary layer climates*. Routledge, London
- Pielke LA (2005) Land use and climate change. *Science* 310(November):1625–1626.
- Sahana M, Ahmed R, Sajjad H (2016) Analyzing land surface temperature distribution in response to land use/land cover change using split window algorithm and spectral radiance model in Sundarban Biosphere Reserve, India. *Model Earth Syst Environ* 2(2):81. doi:[10.1007/s40808-016-0135-5](https://doi.org/10.1007/s40808-016-0135-5)
- Sandholt I, Rasmussen K, Andersen J (2002) A simple interpretation of the surface temperature/vegetation index space for assessment of surface moisture status. *Remote Sens Environ* 79(2–3):213–224. Doi:[10.1016/S0034-4257\(01\)00274-7](https://doi.org/10.1016/S0034-4257(01)00274-7)
- Snyder WC, Wan Z, Zhang Y, Feng Y-Z (1998) Classification-based emissivity for land surface temperature measurement from space. *Int J Remote Sens* 19(14):2753–2774. Doi:[10.1080/014311698214497](https://doi.org/10.1080/014311698214497)
- Sobrino JA, Jiménez-Muñoz JC, Paolini L (2004) Land surface temperature retrieval from LANDSAT TM 5. *Remote Sens Environ* 90(4):434–440. doi:[10.1016/j.rse.2004.02.003](https://doi.org/10.1016/j.rse.2004.02.003)
- Streutker DR (2003) Satellite-measured growth of the urban heat island of Houston, Texas. *Remote Sens Environ* 85(3):282–289. Doi:[10.1016/S0034-4257\(03\)00007-5](https://doi.org/10.1016/S0034-4257(03)00007-5)
- Voogt JA, Oke TR (2003) Thermal remote sensing of urban climates. *Remote Sens Environ* 86(3):370–384. doi:[10.1016/S0034-4257\(03\)00079-8](https://doi.org/10.1016/S0034-4257(03)00079-8)
- Weng Q, Lu D, Schubring J (2004) Estimation of land surface temperature-vegetation abundance relationship for urban heat island studies. *Remote Sens Environ* 89(4):467–483. doi:[10.1016/j.rse.2003.11.005](https://doi.org/10.1016/j.rse.2003.11.005)

- Weng Q, Liu H, Lu D (2007) Assessing the effects of land use and land cover patterns on thermal conditions using landscape metrics in city of Indianapolis, United States. *Urban Ecosyst* 10(2):203–219. doi:[10.1007/s11252-007-0020-0](https://doi.org/10.1007/s11252-007-0020-0)
- Xiao H, Weng Q (2007) The impact of land use and land cover changes on land surface Temperature in a karst area of China. *J Environ Manage* 85(1):245–257. doi:[10.1016/j.jenvman.2006.07.016](https://doi.org/10.1016/j.jenvman.2006.07.016)
- Xiao X, Shen Z, Qin X (2001) Assessing the potential of vegetation sensor data for mapping snow and ice cover: a normalized difference snow and ice index. *Int J Remote Sens* 22(13):2479–2487. doi:[10.1080/01431160119766](https://doi.org/10.1080/01431160119766)
- Xu H (2006) Modification of normalised difference water index (NDWI) to enhance open water features in remotely sensed imagery. *Int J Remote Sens* 27(14):3025–3033. doi:[10.1080/01431160600589179](https://doi.org/10.1080/01431160600589179)
- Xu LY, Xie XD, Li S (2013) Correlation analysis of the urban heat island effect and the spatial and temporal distribution of atmospheric particulates using TM images in Beijing. *Environ Pollut* 178:102–114. doi:[10.1016/j.envpol.2013.03.006](https://doi.org/10.1016/j.envpol.2013.03.006)
- Yuan F, Bauer ME (2007) Comparison of impervious surface area and normalized difference vegetation index as indicators of surface urban heat island effects in Landsat imagery. *Remote Sens Environ* 106(3):375–386. doi:[10.1016/j.rse.2006.09.003](https://doi.org/10.1016/j.rse.2006.09.003)
- Yue W, Xu J, Tan W, Xu L (2007) The relationship between land surface temperatures and NDVI with remote sensing: application to Shanghai Landsat 7 ETM + data. *Int J Remote Sens* 28(15):3205–3226. doi:[10.1080/01431160500306906](https://doi.org/10.1080/01431160500306906)
- Zeng C, Liu Y, Stein A, Jiao L (2015a) Characterization and spatial modeling of urban sprawl in the Wuhan Metropolitan Area, China. *Int J Appl Earth Obs Geoinf* 34:10–24. doi:[10.1016/j.jag.2014.06.012](https://doi.org/10.1016/j.jag.2014.06.012)
- Zeng C, Zhang M, Cui J, He S (2015b) Monitoring and modeling urban expansion—a spatially explicit and multi-scale perspective. *Cities* 43:92–103. doi:[10.1016/j.cities.2014.11.009](https://doi.org/10.1016/j.cities.2014.11.009)
- Zha Y, Gao J, Ni S (2003) Use of normalized difference built-up index in automatically mapping urban areas from TM imagery. *Int J Remote Sens* 24(3):583–594. doi:[10.1080/01431160304987](https://doi.org/10.1080/01431160304987)
- Zhang Y, Odeh IOA, Han C (2009) Bi-temporal characterization of land surface temperature in relation to impervious surface area, NDVI and NDBI, using a sub-pixel image analysis. *Int J Appl Earth Obs Geoinf* 11(4):256–264. doi:[10.1016/j.jag.2009.03.001](https://doi.org/10.1016/j.jag.2009.03.001)
- Zhao HZH, Chen XCX (2005) Use of normalized difference bareness index in quickly mapping bare areas from TM/ETM+. In: *Proceedings. 2005 IEEE international geoscience and remote sensing symposium, 2005. IGARSS'05, vol 3, pp 1666–1668*. doi:[10.1109/IGARSS.2005.1526319](https://doi.org/10.1109/IGARSS.2005.1526319)
- Zhu W, Lú A, Jia S (2013) Estimation of daily maximum and minimum air temperature using MODIS land surface temperature products. *Remote Sens Environ* 130:62–73. doi:[10.1016/j.rse.2012.10.034](https://doi.org/10.1016/j.rse.2012.10.034)